Fall 10-19-2017

Cam-Based Pose-Independent Counterweighting for Partial Body-Weight Support in Rehabilitation

Ashish Shinde

University of Nebraska - Lincoln, ashish.shinde@huskers.unl.edu

Cam-Based Pose-Independent Counterweighting for Partial Body-Weight Support in

Rehabilitation

By

Ashish B Shinde

A THESIS

Presented to the Faculty of

The Graduate College at the University of Nebraska

In Partial Fulfillment of Requirements

For the Degree of Master of Science

Major: Mechanical Engineering and Applied Mechanics

Under the Supervision of Professor Carl Nelson

Lincoln, Nebraska

December 2017

CAM-BASED POSE-INDEPENDENT COUNTERWEIGHTING FOR PARTIAL

BODY-WEIGHT SUPPORT IN REHABILITATION

Ashish B Shinde, M.S.

University of Nebraska, 2017

Advisor: Carl Nelson

This thesis presents the design and testing of a body weight support system for gait training in a two-dimensional workspace. Extension of the system to a three-dimensional workspace is not within the scope of this thesis.

Gait dysfunctions are changes in normal walking patterns, often related to a disease or abnormality in different areas of the body. There are numerous body weight support (BWS) systems present in the market which are applied to rehabilitation scenarios in mobility recovery like in gait training. But most of these BWE systems are costly and generally are stationary devices. A major drawback of such devices is the lack of degrees of freedom for free ambulation. While some multidirectional body weight support systems do exist, these devices are equipped with sensors and control systems which increase the cost of the product.

In this thesis, we introduce a new partial body-weight support system for, and apply this to, a rehabilitation scenario in mobility recovery. The idea behind the research is the development of a low-cost weight-offload system which is easy to operate, flexible in its installation footprint, and requires little to no electromechanical input. We propose a cable-based body-weight support system which allows the user to move in a two-dimensional workspace with a uniform supporting force throughout that workspace. This

is achieved by coupling the cable displacements to the counterweight displacements using mechanical programming via cams. There will be two identical sets of cams, gear boxes, and counterweights to support uniform force on the payload. The system functionality is demonstrated in a prototype embodiment and tested in the lab.

Table of Contents

List of Figures

List of Tables

Abbreviations and Symbols

1. BWS – Body weight support system

2. P – Tension in cable-1 (N)

3. Q – Tension in cable-2 (N)

4. L – (Horizontal) workspace length (m)

5. α – Cable 1 angle with horizontal (radians)

6. β – Cable 2 angle with horizontal (radians)

7. y – Vertical distance of payload, measured from top (m)

8. e– The vertical offset distance between the payload and the cable attachment point (m)

9. x– Horizontal payment displacement

10. W_P – Payload weight (N)

11. L_1/ L_2 – Cable usable lengths for cable 1 & 2

12. t – Time (s)

13. v(t) – The horizontal payload velocity (m/s)

14. x0 – The initial position of the payload (m)

15. κ – Gear box ratio

16. $R(\theta)$ – Cam radius at time t (m)

17. $T_{cable}s$ – Torque acting on the cam from cables (Nm)

18. T_{CW} – Torque acting on the cam provided by the counterweight (Nm)

19. L_{CW} – Counterweight arm length (m)

20. θ – Angle of the counterweight arm length with respect to vertical (radians)

21. L_{Cam} – The effective length of cable wrapped on the cam (m)

22. L_{Cable} – The displacement of cable during payload motion (m)

23. H_P – Reference height of payload on which BWS system is designed (m)

24. R_0 – Initial cam radius (m)

25. E – Young's Modulus of the material (MPa/ psi)

26. S_y – Yield Strength of the material (GPa/ ksi)

27. R_A/R_B – Reactions on the bearings (N)

28. σ_b – Bending Stress in the shaft (N/mm^2)

29. M – Bending Moment in the shaft (Nm)

30. I – Moment of inertia (mm^4)

31. d – Diameter of the gear shafts (mm)

32. SF – Factor of safety

33. Wt – Transmitted load (N)

34. F_w –Net face width of the gear (mm)

35. p – Circular pitch (in)

36. m – module (mm)

37. y, Y –Lewis form factor,

38. σ^g_b – Allowable bending stress in the gear face tooth (N/mm^2)

39. T_{max} – Maximum torque in the gear box system (lb-inch)

40. F_s – Shear force in the key (N)

41. τ – Shear stress in the key (N/mm^2)

42. L_k –length of key (in)

43. b_k – Width and breadth of key (in)

44. W_{spool} – Width of the larger spool (mm /in)

45. d_{fb} – gear box flange bolt diameter (in)

46. N – Number of bolts

47. T_1 – Torque due to the counterweight (Nm)

48. T_2 – Torque due to the payload or tension in the strap (Nm)

49. σ_{allow} – Allowable bending stress in the slotted counterweight arm or shaft

     (N/mm^2)

50. h – breadth of the counterweight arm (in)

51. w – width of the counterweight arm (in)

52. t_{cw} – thickness of the cross section of the counterweight arm (in)

53. $\dot{\theta}$, ω_1 – Angular velocity (rad/s)

54. $\ddot{\theta}$, $\dot{\omega}_1$ – Angular acceleration (rad/s2)

55. v_{cw}, $\dot{r}_{cw}$ – Linear velocity of the counterweight (m/s)

56. r – Radius vector.

57. a_{cw}, $\ddot{r}_{cw}$ – Linear acceleration of the counterweight (m/s^2)

58. F_1 – Net force on the counterweight system (N)

59. e_r – Unit Vector in direction of r

60. e_θ – Unit Vector in direction of θ

61. I_{cw} – Inertial of the counterweight (Nmm^2)

62. v_{cam}, $\dot{r}_{cam}$ – Linear velocity of the cam (m/s)

63. a_{cam}, $\ddot{r}_{cam}$ – Linear acceleration of the cam (m/s^2)

64. F_2 – Net force on the cam (N)

65. e_z – Unit Vector in direction perpendicular to cam

66. e_y – Unit Vector in of gravity

67. I_{cam} – Inertial of the cam (Nmm^2)

68. F_S – Net force/Tension in the strap (N)

69. F_{cam} – Force in cam due to rotation (N)

70. W_{cam} – Weight of the cam (N)

Chapter 1 - Introduction

People with arthritis, stroke or trauma resulting in brain injuries or spinal cord injury (SCI), or other neurological diseases, face problems like loss of motor and sensory ability [1, 2]. Difficulty in walking has an impact on subjects in terms of decreased self-reliance and quality of life [2]. Gait rehabilitation training is commonly employed to regain normal lower-limb function as much as possible [3]. Gait therapy, involving repetitive stepping to restore motor learning and control, is often recommended as a part of the rehabilitation process; this may be complemented by balance therapy and various forms of occupational therapy [4].

1.1. Gait Dysfunctions

Gait dysfunctions are changes in your normal walking pattern, often related to a disease or abnormality in different areas of the body. Individuals with gait dysfunctions may have a gait pattern characterized by hesitant, shuffling steps that are short and quick. Gait dysfunctions cause difficulties in gait initiation, changes in postural control, and difficultly in turning. Freezing and motor blocks, balance deficits and frequent falls occur during later stages of gait dysfunction [5]. Gait and balance disorders are associated with increased morbidity and mortality, as well as reduced level of function. Gait dysfunctions are commonly caused by spinal cord injuries, stroke, Parkinson's disease, arthritis, orthostatic hypotension, etc.; however, most gait and balance disorders involve multiple contributing factors [6, 7].

Gait training is a method to reduce mobility dysfunction. Gait training can be used to treat diverse patient populations that exhibit mobility impairments. Two such populations are people with post-stroke and post-spinal cord injury. Gait training or locomotion therapy uses several devices to assist the patient with moving and maintaining balance [8]. These include treadmill training with partial body-weight support [9], robotically assisted gait repetition [10], and other devices such as elliptical machines which combine robotic assistance with body-weight support features [11, 12, 13, 14, 15]. Gait training is a type of physical therapy that can help improve patients' ability to walk, typically relying on such devices.

There are numerous secondary benefits to gait training. Many medical and psychosocial problems occur when subjects are bound to a wheelchair or bed for a lengthy period. According to Frey et al. [16], "Some of the most common problems are pressure sores, reduced bone-density in the legs, increased risk of fractures, deterioration of cardiopulmonary and circulatory functions, spasticity, bowel and bladder stagnation, urinary tract infections, and joint contractures." Treadmill training provides exercise and mobility that offer some solutions to these problems [16].

1.2. Body Weight Support System (BWS)

Body weight support (BWS) systems are used to assist therapists in gait training of patients with gait dysfunctions. The main purpose of BWS is to unload part of patients' weight to accommodate patients' weakness and to facilitate safe therapy. It works on the principle of reducing the muscle force required to counteract gravity [17]. Body weight support (BWS) exerts forces on an individual that could change the requirements of the

nervous system to actively stabilize the body during gait [17]. To utilize BWS effectively, it is important to understand the implementation and force mechanism of BWS [17].

A major design challenge for designing BWS is to overcome slow walking speeds and increased risks for falls. Reliability and safety of the BWS is very important. Another important challenge in designing a BWS is adjustability. It should adapt to changes in force requirements. It should provide appropriate mechanical assistance to patients while walking [18].

1.3.   Overview of Bodyweight Support Systems

A BWS system in gait therapy consists of a harness system worn by patients and a method of unloading part of a patient's weight (e.g. ropes and pulleys and a counterweight); hereafter this partial patient weight is referred to as payload. The use of treadmill-based BWS began in the early 1990s [19]. Following are existing BWS systems [16]:

1.3.1. Treadmill Bodyweight Support Systems

Perhaps the most common type of BWS system is with one or two degrees of freedom while patients walk on a treadmill. Major drawbacks of such systems are limited degrees of freedom and/or undesired interaction forces due to inertia [16]. Also, patients have to continuously adjust their walking velocity to maintain their position on the treadmill [20].

A.   Static Systems

A static system is shown in Figure 1-1 (A). In this system, a harness is attached to an overhead suspension composed of ropes and pulleys. The ropes are connected to a winch

for counterweighting the payload. The winch can be actuated either manually or automatically using electric or hydraulic drives. The winch wraps the rope until it supports the desired payload. More advanced systems use a transducer for weight feedback during hoisting. The main disadvantage of this system is the limited vertical movement of the center of mass. Thus, the constant potential energy of the payload is not maintained which may hamper the execution of gait patterns [16].

B.   Passive Dynamic BWS with Adjustable Counterweights

An adjustable system is shown in Figure 1-1 (B). The counterweight can be used for the balancing of payload or dynamically unloading part of the patients' body weight. It is connected to the patient harness by a rope-and-pulley system. It comprises weight and an inertial component, resulting from acceleration of the counter-mass from body movement during walking. These inertial forces cause deviations of the suspension force from the desired value. Also, only a discrete value of counterweight can be achieved [16].
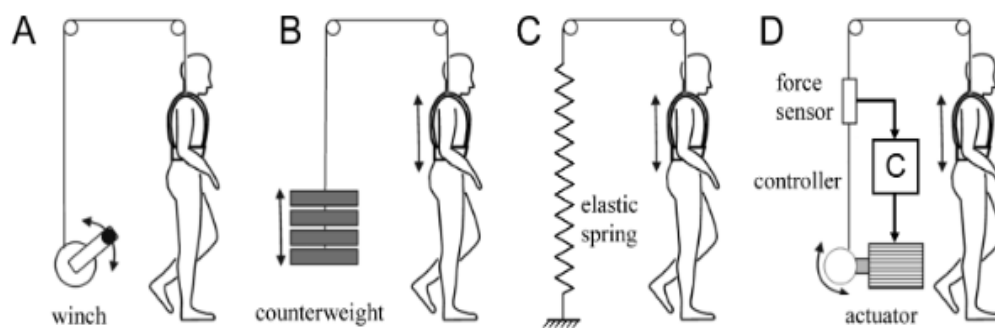
Figure 1-1 Overview of body weight support systems [16]

(A) Static BWS. (B) Passive counterweight systems. (C) Passive elastic systems (spring). (D) Active dynamic system with force sensor and electric winch

5

C.   Passive Dynamic Elastic Systems

An elastic system is shown in Figure 1-1 *(C)*. Elastic components can be used for counterweighting the payload. The amount of unloading is determined by the amount of tension of the elastic element. Passive elastic unloading can also be achieved by pneumatic cylinders filled with compressed air. The advantage of this system compared to the earlier one is that inertial effects can be neglected. However, suspension force is a function of spring length and therefore varies due to the vertical movement of the patient. Low-stiffness springs can be used to reduce force variation. However, this results in a long spring elongation to obtain the desired working load. Drawbacks of such systems include difficulty of load adjustments over a large range [16].

D.   Active Dynamic Systems

An active system is shown in Figure 1-1 (D). Active dynamic systems like pneumatic, hydraulic, and electromagnetic or any other force generating system which produces a desired force to counterweight the payload, can be used in body weight support systems. The vertical position of the supporting force to the patient's movement is adjusted by applying a closed loop approach in which a position sensor measures the vertical position. This feedback is given to the actuator to generate desired positions or forces [16].

E.   Mechatronic Body Weight Support System

A mechatronic system is shown in Figure 1-2. The mechatronic BWS combines key ideas of both passive elastic and active dynamic systems. The system is composed of a passive elastic spring element to take over the main unloading forces, and an active

dynamic system like a closed loop electric drive to generate the exact desired force. These

forces from passive spring and active electric drive act on the patient via a rope connected

to a harness worn by the patient. The length of the rope can be adjusted by an electric winch

to adapt the system to different patient sizes. The patient is placed in a harness via the rope.

The rope is guided via static pulleys seated by ball bearings. The end of the rope is attached

to the electric winch which serves to lift the patient from a static position as well as keep

the system in an optimal working range [16].
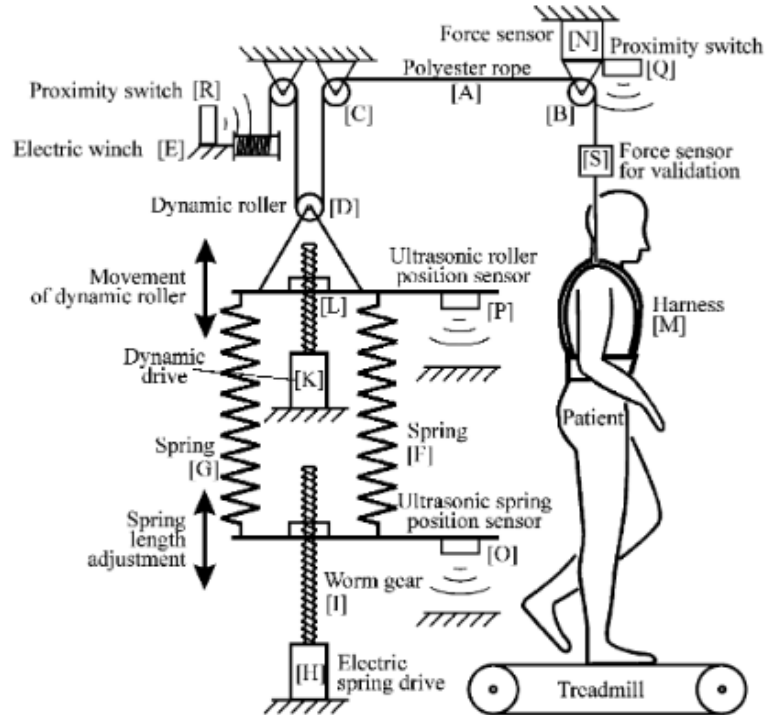
Figure 1-2 Mechatronic body weight support system [16]

A major drawback of BWS treadmills, apart from the limited degrees of freedom,

is the high equipment cost and the labor-intensive nature of the system. Major sellers of

BWS treadmills sell devices ranging from $10,000 to $15,000. Integrated BWS treadmills

may cost up to $180,000 [21].

1.3.2.   Multidirectional Transparent Support System

The robotic system FLOAT (Free Levitation for Overground Active Training) is an overhead support system that is designed to precisely control forces acting on a human subject in vertical and in both horizontal directions, (Figure 1-3). The device capitalizes on cable robot technology that allows three-dimensional gait training. It reduces the effects of inertial forces on the system. The FLOAT allows the patients to move in a large workspace, so diverse activities can be trained and analyzed in patients such as level walking, running, walking on uneven terrain and stair climbing. Two parallel rails are arranged on the ceiling, which guide two deflection units each. Each deflection unit (refer to Figure 1-3) is composed of a rolling cart carrying an inclinable pulley. At each end of the rails, a winch with a laser sensor is positioned. From each winch, cable extends via the deflection unit which is harnessed to the patient. The force vector acting on the human (payload) is used to implicitly displace the deflection unit in the horizontal direction along the rail [22].
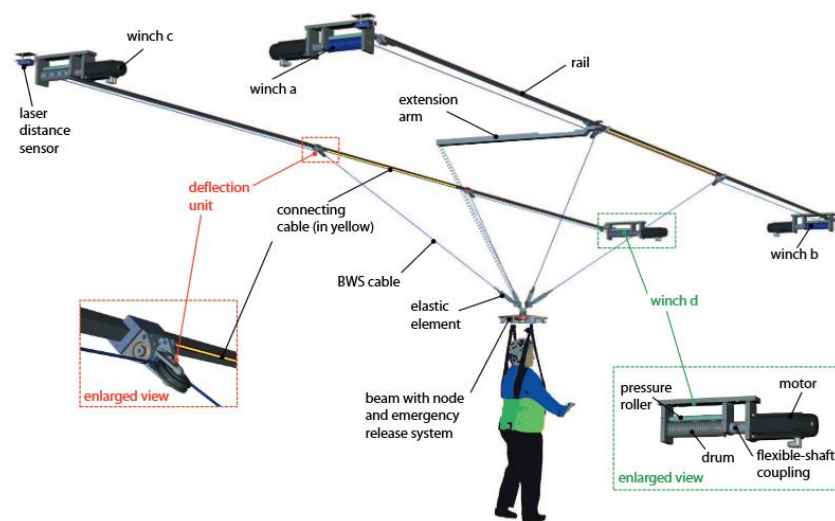
Figure 1-3 Concept of FLOAT body weight support system [22]

1.4.   Summary and Problem Approach

Gait dysfunctions are changes in normal walking patterns, often related to a disease or abnormality in different areas of the body. Gait training uses several devices to assist the patient to move and maintain balance. There are numerous body weight support (BWS) systems to address the need of gait rehabilitation, such as the treadmill body weight support system [16], the multidirectional transparent support system [22], passive suspension walkers [15], and robotically mobilized walkers [13]. Treadmills with un-weighting devices are used to train walking at various speeds on a straight flat surface or a small incline. Drawbacks of these BWS systems include high cost and they generally are stationary devices. More drawbacks of devices similar to treadmills include the limited degrees of freedom for free ambulation. There are some multidirectional BWS systems that exist and are equipped with sensors and control systems which increase the cost of the product.

A primary idea would be a partial body-weight support system which bridges the gap between stationary assistive devices like treadmills and the subsequent phases of rehabilitation involving more advanced mobility [11]. The requirement for such a system is to provide consistent body-weight support throughout a planar "workspace" during gait rehabilitation [11]. This proposed system should equip the entire space (rather than the patient) with a cable system, like a cable-suspended robot [23], suitable for attaching a typical body-weight support harness used with other rehabilitation devices. This proposed

system can be tuned to passively compensate for a portion of the weight of the patient as needed for his/her individualized therapy to keep the system discreet and affordable [11].

The generation of three-dimensional workspace will be complicated. The approach used in this thesis is to build the system in a two-dimensional workspace, verify the concept by developing the prototype in the lab for design parameters discussed in this thesis, and suggest necessary modifications for the system. Therefore, this thesis consists of designing and testing a partial body-weight support system in a two-dimensional workspace. Although a reduction in cost of existing BWS systems is one of the design objectives, we will not consider that in the current phase. Our focus is on verification and validation of the proposed idea in a two-dimensional workspace.

1.5.   New Partial Body Weight Support System Design Requirements

The following are the design requirements of a new partial body-weight support system.

A.   3-Dimensional Workspace

The main disadvantage of treadmills is the limited degrees of freedom. Therefore, while designing the new system, we must consider that the patient should be able to walk throughout a room. The device must allow the patient to move freely without constraining him or her.

B.   Simplified System Controls

For simplicity, there should be less use of controls and sensors, and ideally the design should be purely mechanical. This will reduce the cost of the system as well as potential failure points.

C.   Safety

Gait simulators are usually complex robotic devices on which the patient stands and moves. To avoid accidents, the BWS device must be constrained to move only within the physiological limits of the human body. It also must provide the patient with the means to quickly reach safety should anything wrong happen with the system.

Since the proposed partial BWS could eventually be marketed as a medical device, it should comply with relevant safety standards such as International Standard IEC 60601-1 [19].

Chapter 2 - Modeling Approach

To satisfy the design objectives given in section 1.4 and the design requirements given in section 1.5, a two-dimensional workspace is considered in which the patient walks along a straight line. Using a planar system of two cables suspended from two anchoring points, one can fully balance a load vertically while maintaining zero net force on the payload horizontally (see *Figure 2-1*). The necessary cable tensions are related through a nonlinear function which can be "programmed" mechanically, without any actuators or control, only using stored energy in a system of counterweights. This concept of static balancing has been applied in a variety of systems using springs, counterweights, and other means [24, 25, 26]. Here we used a mechanical device, a cam with a torsional counterweight, as a function generator to map the nonlinear relation between the cable tension and cable displacement such that equilibrium was maintained.

2.1. Balancing of Payload

Referring to Figure 2-2, let the tension in cable 1 be P (N), and let the tension in cable 2 be Q (N). With the distance between the columns equal to L, and the payload located at a distance y, measured vertically from the tops of the columns, the condition constraining the payload to remain at a constant height is given by,

$$\cot\alpha + \cot\beta = \frac{L}{y - e} \qquad (1)$$

where e is the vertical offset distance between the payload and the cable attachment point, and α and β are the respective cable angles.
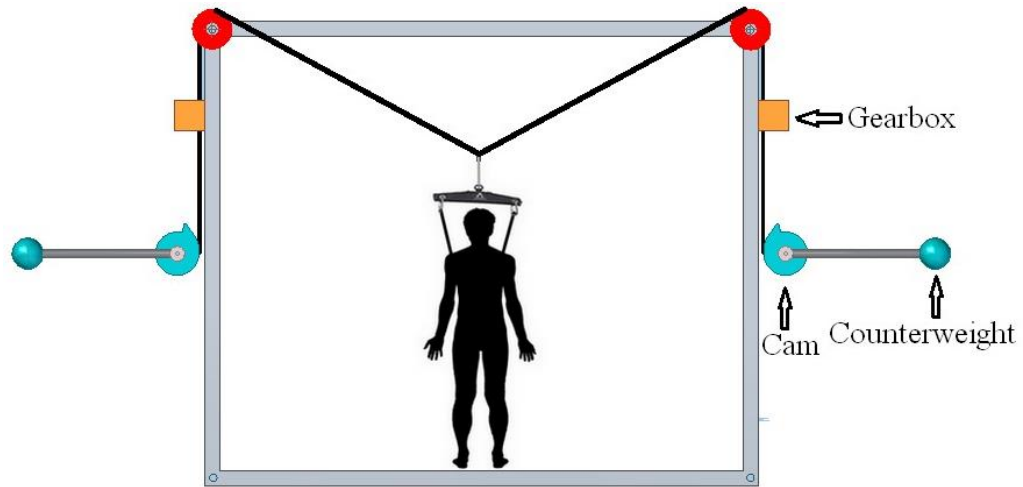
Figure 2-1 System layout
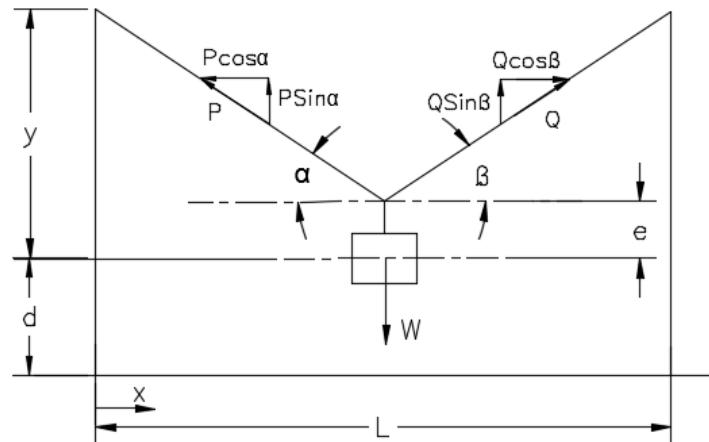
Figure 2-2 Schematic of forces, angles and displacements

Applying principles of static force equilibrium, balancing the horizontal forces gives:

$$P\cos\alpha = Q\cos\beta \qquad (2)$$

and balancing the vertical forces yields:

$$P\sin\alpha + Q\sin\beta = W_p \qquad (3)$$

where W_P is the payload weight. Solving these two simultaneous equations (2) and (3),

we obtain the tension in each cable:

$$P = \frac{W_P \cos\beta}{\cos\alpha \sin\beta + \cos\beta \sin\alpha} = \frac{W_P \cos\beta}{\sin(\alpha + \beta)} \qquad (4)$$

$$Q = \frac{W_P \cos\alpha}{\cos\alpha \sin\beta + \cos\beta \sin\alpha} = \frac{W_P \cos\alpha}{\sin(\alpha + \beta)} \qquad (5)$$

Using the position coordinates to substitute for the angles gave an alternate form of

the tension expressions in terms of the horizontal payload displacement x:

$$Q = \frac{W_P x \sqrt{(L-x)^2 + (y-e)^2}}{L(y-e)} \qquad (6)$$

The relation between the tensions P and Q in the cable and the horizontal payload

distance can be shown graphically. We considered width of the workspace (L) (3.64 m)

and a specific payload (W_p) (100 kg) and height (d) (2 m); this relationship is shown in

Figure 2-3. We also note that P is symmetric with Q.

Extending this relationship to the entire workspace of the system (3.64 m wide and

up to a height of 3.05 m), one obtains the distribution in Figure 2-4.

Besides showing the nonlinear variation of the cable tension as a function of the

horizontal and vertical coordinates, Figure 2-4 brings to light significant increase of the

cable tension for payload levels over two meters.

Using the Pythagorean Theorem, cable usable lengths are given by:

$$L_1 = \sqrt{x^2 + (y-e)^2} \qquad (7)$$

$$L_2 = \sqrt{(L-x)^2 + (y-e)^2} \qquad (8)$$
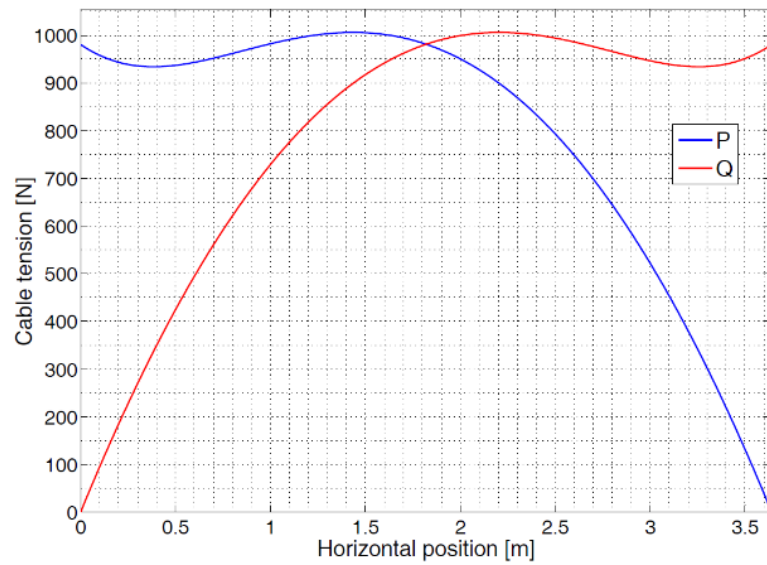
Figure 2-3 Cable tension for a 100-kg payload at a 2-meter payload height
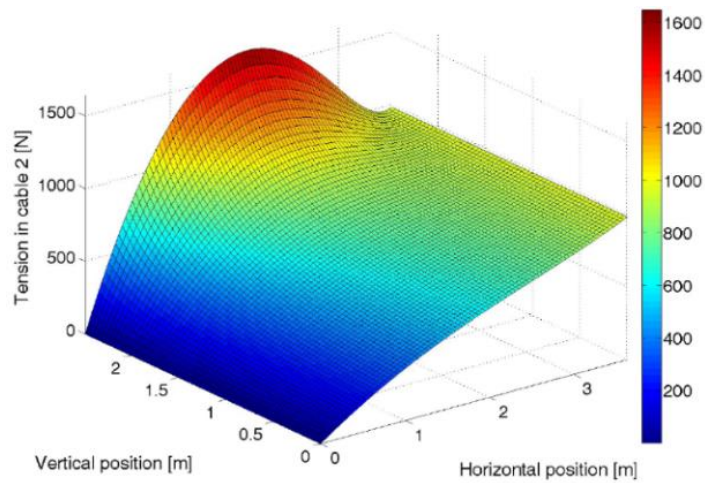
Figure 2-4 Cable 2 tension depending on payload (100 kg) position

Considering the actual workspace dimensions, this relationship led to the cable displacement shown in Figure 2-5.

Differentiating those expressions with respect to the horizontal position yielded expressions for rates of change of the cable length depending on x position (with y assumed

fixed). As noted earlier, the displacements and speeds were symmetric, depending on whether the right or left cable origin was used as the reference frame.

$$\frac{dL_1(x)}{dx} = \frac{x}{\sqrt{(y-e)^2 + x^2}} \qquad (9)$$
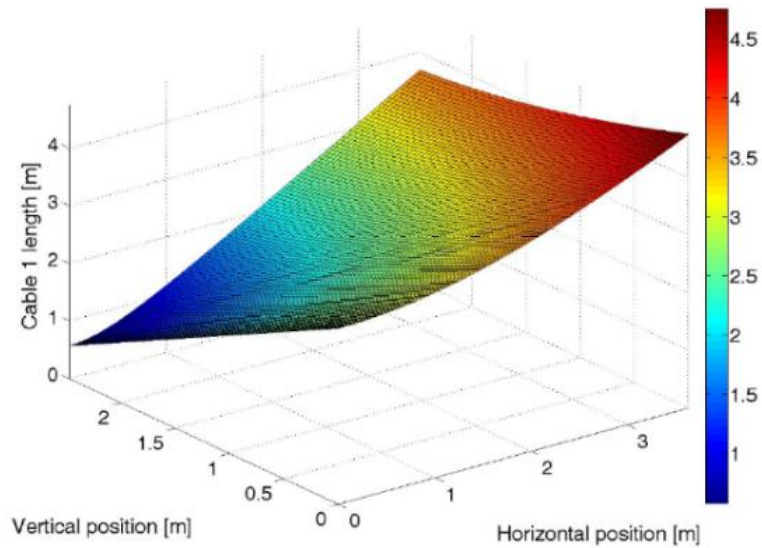
Figure 2-5 Cable 1 length depending on payload position

Applying the chain rule (multiplying Equation (9) by *x*-velocity) gives the general shape of the cable tangential speed profiles as shown in Figure 2-6, as the horizontal position (*x*) is a function of horizontal payload velocity:

$$\frac{dL_1(x)}{dx} = \frac{x}{\sqrt{(y-e)^2 + x^2}} \qquad (10)$$

where *v*(*t*) is the horizontal payload velocity, x_0 the initial position and *t* the time.
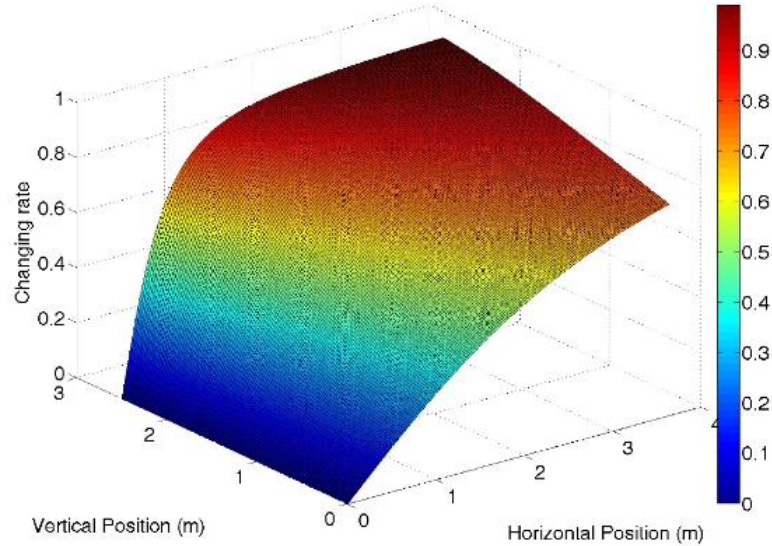
Figure 2-6 Cable 1 speed depending on payload horizontal position

2.2.   Counterweight System Design

The counterweight system was designed to follow the tensile force profiles in the cables as a function of cable displacement. It consisted of a gearbox, cam, and pendulum counterweight. The gearbox allowed scaling of the cable displacement (on the length scale of the workspace) down to the length scale of the cam circumference. The varying cam radius combined with the sinusoidal moment produced by the counterweight arm to match the nonlinear cable displacement-tension profile. This arrangement is shown in *Figure 2-1*

Since the cam was a 1-DOF function generator, it could only be used to balance the system in 1 DOF. Therefore, since cable tension varies with both horizontal displacement and payload height (*Figure 2-4*), the counterweight system would theoretically only be able to balance the payload for the reference height (H_P) for which it has been designed. In other cases, motors would have to provide additional torque in order to maintain equilibrium.

The cam shape was synthesized as follows. Considering the left cable shown in Figure 2-2 with tension P (given in (4)), the torque acting on the cam from the cable is given by:

$$T_{cables} = \kappa \times P \times R(\theta) \tag{11}$$

where κ is the gearbox ratio and $R(\theta)$ the cam radius at time t.

The torque provided by the counterweight is given by the following equation:

$$T_{CW} = W_{CW} \times L_{CW} \times \sin\theta \tag{12}$$

where W_{CW} is the counterweight (N), L_{CW} the arm's length (m) to which the counterweight is attached, and θ is the angle (rad) of the counterweight arm with respect to the vertical. For a fully balanced system, one obtains:

$$W_{CW} \times L_{CW} \times \sin\theta = \kappa \times P \times R(\theta) \tag{13}$$

We noted that $R(\theta)$ is an as-yet unknown function of θ at time t.

The effective length of cable wrapped on the cam is given by:

$$L_{CAM} = \kappa \int R(\theta) d\theta \tag{14}$$

Considering the reference payload's level (two meters), this length should match the displacement of cable length during payload motion:

$$L_{Cable} = L_i - L_x = \sqrt{L^2 + (y - e)^2} - \sqrt{x^2 + (y - e)^2} \tag{15}$$

The effective length of cable wrapped should be equal to the displacement of cable length during payload motion.

$$L_{Cable} = L_{CAM} \tag{16}$$

Therefore,

$$\kappa \int R(\theta)d\theta = \sqrt{L^2 + (y-e)^2} - \sqrt{x^2 + (y-e)^2} \qquad (17)$$

2.3. Cam Design

Cam design was difficult to derive due to the implicit nature of equations (11), (12), (14), and (15). Here $R(\theta)$ implicitly depends on $\sin\theta$, i.e. the counterweight arm angle with respect to horizontal and cable tensions (P or Q) (refer to equation (13)). Furthermore, by equation (17), $R(\theta)$ depends on x.

By equation (17),

$$x = \sqrt{(\sqrt{L^2 + (y-e)^2} - (\kappa \int R(\theta)d\theta)^2 - +(y-e)^2} \qquad (18)$$

From (6), we can see that cable tension, P (or Q) depends on payload displacement x.

$$P = \frac{W_P(L-x)\sqrt{(x)^2 + (y-e)^2}}{L(y-e)} \qquad (19)$$

Rewriting (13),

$$\frac{W_{CW} \times L_{CW} \times \sin\theta}{\kappa \times R(\theta)} = P \qquad (20)$$

2.3.1. Trial and Error Approach

Since we observed that equations (18), (19) and (20) are implicitly interdependent, we could not solve these equations for the three variables x, $R(\theta)$ and θ. These equations can be solved numerically. One of the easiest ways to solve these equations is a trial and error method. The basic idea behind this method is to assume an initial value of one of the variables and solve all equations for the remaining variable. Since we assumed one of the variables, the solution would not satisfy all the equations. We either increased the value of an assumed variable or decreased it and compared the difference in solutions [27]. This

process was continued until all the equations were satisfied with a certain degree of error. We used MS-Excel for carrying out these iterations.

2.3.2. Initialization for R(θ).

All iterations were done by initializing $R(\theta)$ and then calculating the gear box ratio by using equation (21).

Due to the implicit nature of the equations, we assumed $R(\theta)$ (denoted as R_0) to be some constant value related to the gear box ratio:

$$R_0 \geq \frac{\sqrt{L^2 + (y-e)^2} - (y-e)}{\kappa \times \pi / 2} \qquad (21)$$

Here rotation of the cam was restricted to 90°. This restriction was necessary, since the sine function varies from 0 to 1 in 90°. The gear box ratio and the initial value were both considered by taking into account the size of the resulting cam. If we assumed a gear box ratio as low as five, then the resulting cam would be too big and the purpose of gear box would not be served.

2.3.3. Design Parameters for Cam Design:

For designing the BWS, we assumed some parameters to be fixed so we could build the system. The cam profile was checked by changing one of these parameters and observing its effects on other variables. See Table 2 1.

A. Payload (W_P):

The cam was designed for a payload of 150 kg. But the BWS system factor of safety was calculated by considering a maximum payload of 200 kg.

Table 2-1. Design parameters

Parameters	Value
Payload $(W_P)^A$	150 kg
Length of Workspace (L)	3.65 m
Height of Workspace (H)	3.05 m
Payload height from top (H_P) (Reference Height) [B1]	1.05 m
Payload height from top (y-e) (Case 2) [B2]	1.35 m
Payload height from top (y-e) (Case 3) [B3]	0.75 m
Length of counter weight Arm (L_{CW})	1 m
Gear Box Ratio $(\kappa)^C$	12
Counterweight $(W_{CW})^D$	400 kg

B.   Payload Height from top (*y-e*):

For designing the cam, the payload vertical location is important. Since displacement of cable length and tension in the cables are dependent on the vertical location of the payload, it is important to consider an increase or reduction in payload. For design of the cam, we considered three cases for payload location – 0.75 m, 1.05 m and 1.35 m. The cam was designed for a reference height of 1.05 m.

C.   Gear box ratio:

Initially the gear box ratio was assumed to be 10. But since the actual profile of the cam was non-circular and different from the initially assumed profile, there was a change in the gear box ratio. The gear box ratio was calculated as,

$$\kappa \geq \frac{\sqrt{L^2 + (y-e)^2} - (y-e)}{\int_0^{\pi/2} R d\theta} \qquad (22)$$

D.   Counterweight:

The counterweight was calculated from (13) as,

$$W_{CW} = \frac{\kappa \times P_{max} \times R(t)}{L_{CW} \times \sin\theta} \qquad (23)$$

The maximum counterweight depends on the maximum tension in the cables, the radius of the cam at that point, and the angle of the counterweight arm.

2.3.4. Cam design - Iteration 1:

These iterations were carried out by assuming x in steps:

1. We discretized the workspace length L into small intervals, and calculated P & Q using equations (18) & (6) at each discrete location. For example, in Table 2-2 , x is discretized into 14 points, each 0.26 m in length.

2. Simultaneously, we calculated the displacement of cable 1 (L_1) and cable 2 (L_2) using equation (15).

3. We assumed a circular profile for the cam and initial radius R_0 calculated by (21); R_0 came out to be 0.2 m.

4. We calculated the position of the counterweight arm (θ) using (13). In this step, we balanced the torque provided by the counterweight with the torque required by the cables.

5. We obtained the length of cable wrapped by the cam as $L_{CAM} = \kappa R\theta$.

6. The results are shown in Table 2-2.

Table 2-2. Iteration 1- cam design parameters for initial cam radius

Movement of Payload(x)	T_{Cable1} P (N)	Cam Radius (m)	CW Angle (θ)(Rad)	L_{cam} (m)	L_1 (m)
0	1500	0.2	1.063	0.213	0.274
0.26	1434.92	0.2	0.990	1.979	0.271
0.52	1434.74	0.2	0.989	1.979	0.262
0.78	1468.18	0.2	1.026	2.052	0.248
1.04	1508.03	0.2	1.073	2.145	0.231
1.3	1534.66	0.2	1.106	2.212	0.212
1.56	1535.06	0.2	1.107	2.213	0.191
1.82	1500.83	0.2	1.064	2.128	0.169
2.08	1426.53	0.2	0.981	1.962	0.146
2.34	1308.56	0.2	0.867	1.734	0.122
2.6	1144.5	0.2	0.730	1.459	0.098
2.86	932.65	0.2	0.574	1.149	0.074
3.12	671.83	0.2	0.402	0.804	0.050
3.38	361.16	0.2	0.212	0.424	0.025
3.64	0	0.2	0.000	0.000	0.000

7. In the above steps, we have balanced the torque provided by the counterweight with the torque required to balance the payload. But the length of cable wrapped by the cam was not equal to the displacement of the cable in the workspace. That is, equation (17) was not satisfied. We tried to achieve this equilibrium by changing R_0, so that it was satisfied. The results are shown in Table 2-3.

8. The cam radius from Table 2-3 is plotted in Figure 2-7. With these points (iterated cam profile radius) we fit a polynomial of degree six which came out to be:

$$R(t) = -7 \times 10^{-08} \times x^6 + 5 \times 10^{-06} \times x^5 - 0.0001 \times x^4 + 0.0017 \times x^3$$
$$- 0.012 \times x^2 + 0.032 \times x + 0.1962$$

(24)

Table 2-3. Cam radius after iteration 1.8

Cam Radius (m)	CW Angle (θ)(Rad)	L_{cam} (m)	L_1 (m)
0.218	1.258	2.738	2.738
0.224	1.209	2.706	2.707
0.221	1.182	2.616	2.617
0.214	1.158	2.480	2.480
0.205	1.125	2.310	2.311
0.197	1.076	2.117	2.117
0.189	1.008	1.908	1.908
0.183	0.924	1.687	1.687
0.177	0.825	1.458	1.458
0.172	0.713	1.223	1.224
0.167	0.590	0.984	0.984
0.162	0.457	0.742	0.742
0.158	0.314	0.496	0.496
0.154	0.162	0.250	0.249
0.150	0.000	0.000	0.000

9. Equation (24) is the trendline from Figure 2-7. This polynomial plot was used for modeling and manufacturing the cam since it is difficult to model the cam with discrete points.
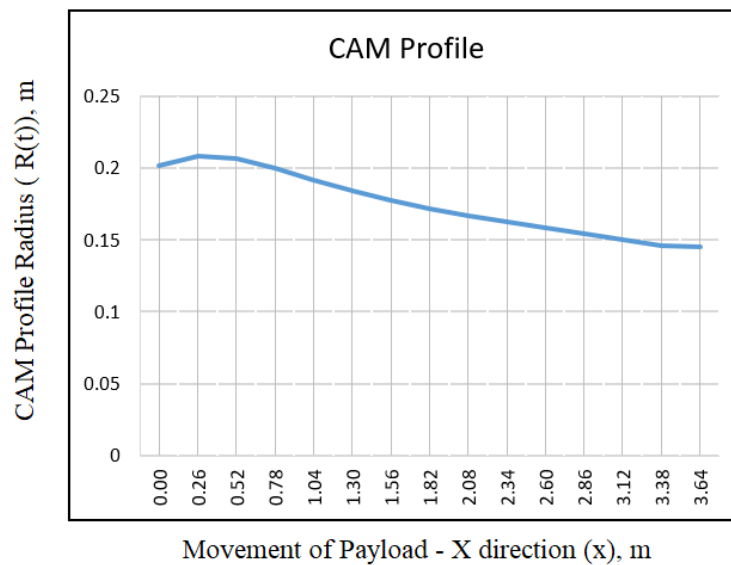
Figure 2-7 Cam radius plot vs x(t)

Table 2-4. Verification of cam profile radius after iteration 1

Sr. No	X	P	R(θ)	Theta	L$_1$	T$_{CW}$	L$_{cam}$	T$_{cable1}$	T$_{cw}$-T$_{cable}$	L$_{cw}$-L$_{cable}$
0	0.00	1500.00	0.196	1.030	2.738	2943.000	2.340	2943.000	0.000	0.398
1	0.26	1434.92	0.204	1.019	2.707	2923.488	2.319	2923.488	0.000	0.388
2	0.52	1434.74	0.210	1.069	2.617	3010.483	2.421	3010.483	0.000	0.195
3	0.78	1468.18	0.215	1.162	2.480	3151.157	2.617	3151.157	0.000	-0.137
4	1.04	1508.03	0.218	1.283	2.311	3292.062	2.875	3292.062	0.000	-0.565
5	1.30	1534.66	0.221	1.414	2.117	3391.414	3.162	3391.414	0.000	-1.045
6	1.56	1535.06	0.223	1.484	1.908	3420.483	3.316	3420.483	0.000	-1.408
7	1.82	1500.83	0.224	1.365	1.687	3360.964	3.051	3360.964	0.000	-1.364
8	2.08	1426.53	0.224	1.201	1.458	3201.970	2.685	3201.970	0.000	-1.227
9	2.34	1308.56	0.224	1.027	1.224	2937.666	2.293	2937.666	0.000	-1.069
10	2.60	1144.50	0.224	0.844	0.984	2565.524	1.882	2565.524	0.000	-0.898
11	2.86	932.65	0.224	0.653	0.742	2085.048	1.454	2085.048	0.000	-0.712
12	3.12	671.83	0.223	0.451	0.496	1496.802	1.003	1496.802	0.000	-0.507
13	3.38	361.16	0.222	0.236	0.249	801.629	0.523	801.629	0.000	-0.274
14	3.64	0.00	0.221	0.000	0.000	0.000	0.000	0.000	0.000	0.000

10. We could see that error in recalculations of the length of cam to be wrapped and the length of displacement of the cable was excessive. We decided not to use this approach. Also, here the cam radius was a function of x and not θ, so we needed to create one more approximation for $R(\theta)$ as a function of θ. This approximation would generate error.

2.3.5. Cam design - Iteration 2:

These iterations were carried out by discretizing the cam profile (θ). Also design of the cam profile was restricted to the range 0 to 90˚.

1. The first step was to discretize the cam profile. That is, θ was divided into 90 intervals from 0 to 90˚.

2. We calculated the torque provided by the counterweight T_{CW} by using (12).

3. We assumed a circular profile for the cam and an initial radius R_0 calculated by equation (21). R_0 came out to be 0.2 m.

4. We obtained the length of cable wrapped by the cam as $L_{CAM} = \kappa R \theta$.

5. We calculated the position of the payload x in the workspace by using (18).

6. We calculated cable tensions P and Q by using (5) and (19).

7. We calculated the displacement of cables (L_1 and L_2) from the payload position using (15).

8. We calculated the torque provided by the cable T_{cable} by using equation (11).

9. The results are shown in **Table 2-5**.

Table 2-5. Cam design – iteration 2 for initial radius 0.2m

Sr No.	Theta	T$_{CW}$	Initial R	L$_{cam}$	X	P	L$_1$	T$_{cable\ 1}$
0	0.000	0.000	0.2	0.000	3.640	0.000	3.788	0.000
5	0.087	341.999	0.2	0.209	3.421	306.927	3.579	736.626
10	0.175	681.395	0.2	0.419	3.202	579.536	3.370	1390.886
15	0.262	1015.606	0.2	0.628	2.981	817.859	3.160	1962.862
20	0.349	1342.087	0.2	0.838	2.758	1021.944	2.951	2452.666
25	0.436	1658.354	0.2	1.047	2.532	1191.860	2.741	2860.465
30	0.524	1962.000	0.2	1.257	2.304	1327.713	2.532	3186.510
35	0.611	2250.714	0.2	1.466	2.071	1429.665	2.322	3431.196
40	0.698	2522.299	0.2	1.676	1.834	1497.991	2.113	3595.179
45	0.785	2774.687	0.2	1.885	1.588	1533.183	1.903	3679.638
50	0.873	3005.958	0.2	2.094	1.329	1536.212	1.694	3686.908
55	0.960	3214.353	0.2	2.304	1.050	1509.335	1.485	3622.404
60	1.047	3398.284	0.2	2.513	0.724	1459.545	1.275	3502.909
65	1.134	3556.352	0.2	2.723	0.182	1446.198	1.066	3470.875

10. For equilibrium of forces and torque, equation (13) should be satisfied. That is, torque provided by the counterweight should be equal to the torque due to tension in the cables. We tried to achieve this equilibrium by changing R_0, so that it was satisfied.

11. The results are shown in Table 2-6.

Table 2-6. Cam design – iteration 2 after recalculated $R(\theta)$

Sr No.	Theta	T_{CW}	Initial R	L_{cam}	X	P	L_1	T_{cable1}
0	0.000	0	0.133	0	3.64	0	3.788	0
1	0.017	68.483	0.133	0.028	3.611	42.833	3.761	68.413
2	0.035	136.946	0.134	0.056	3.582	85.246	3.733	136.769
3	0.052	205.366	0.135	0.084	3.552	127.294	3.704	205.453
4	0.070	273.724	0.135	0.112	3.523	168.874	3.676	273.576
5	0.087	341.999	0.136	0.141	3.493	210.009	3.648	341.726
10	0.175	681.395	0.139	0.285	3.343	408.935	3.504	680.632
15	0.262	1015.606	0.142	0.432	3.188	595.714	3.356	1015.096
20	0.349	1342.087	0.145	0.583	3.029	769.236	3.205	1342.164
25	0.436	1658.354	0.149	0.737	2.865	928.435	3.051	1656.700
30	0.524	1962.000	0.153	0.896	2.696	1072.216	2.893	1962.155
35	0.611	2250.714	0.156	1.058	2.521	1199.431	2.731	2251.092
40	0.698	2522.299	0.161	1.224	2.340	1308.781	2.564	2522.283
45	0.785	2774.687	0.165	1.395	2.151	1398.897	2.393	2774.852
50	0.873	3005.958	0.171	1.571	1.953	1468.226	2.217	3005.752
55	0.960	3214.353	0.177	1.754	1.743	1515.014	2.034	3214.254
60	1.047	3398.284	0.184	1.944	1.517	1537.212	1.845	3397.853
65	1.134	3556.352	0.193	2.142	1.268	1532.594	1.646	3556.844
70	1.222	3687.354	0.205	2.352	0.981	1499.524	1.437	3688.828
75	1.309	3790.293	0.219	2.575	0.609	1443.865	1.214	3791.013

12. These iterated points we plotted as $R(\theta)$ vs θ as shown in Figure 2-8. With these points (iterated cam profile radius) we fit a polynomial of degree six which came out to be:

$$R(\theta) = -0.0708\theta^6 + 0.2856\theta^5 - 0.404\theta^4 + 0.2702\theta^3 \\ - 0.078\theta^2 + 0.0447\theta + 0.1323 \tag{25}$$

13. Equation (25) is the trendline from Figure 2-8. This polynomial plot was used for modeling and manufacturing the cam since it is difficult to model the cam with discrete points.

14. Validation of Design:

The final cam radius needed to be verified, since we had a plot of the trendline which deviated from the actual cam profile. This deviation was measured in terms of the difference in torque provided by the counterweight and torque resulting from the cable tensions and the difference in length of cable wrapped on the cam, from the displacement of cable in the workspace. See Table 2-7.
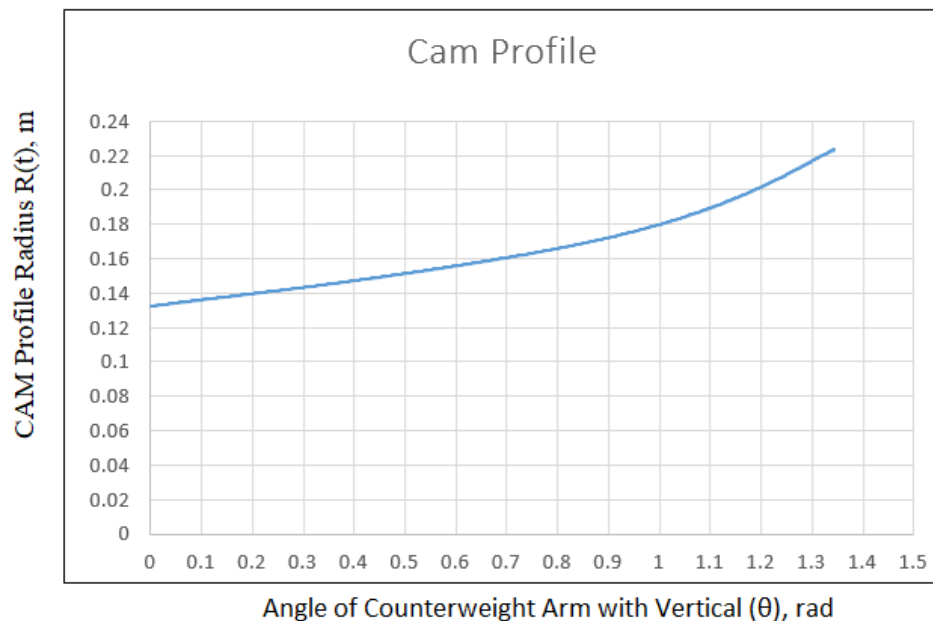
Figure 2-8 Cam radius plot vs counterweight arm rotation

Table 2-7. Verification of corrected $R(\theta)$

Sr No.	Theta	T$_{CW}$	$R(\theta)$	L$_{cam}$	X	P	L$_1$	T$_{cable1}$	T$_{cw}$-T$_{cable1}$	L$_{cw}$-L$_1$
0	0.000	0.000	0.132	0.000	3.640	0.000	0.000	0.000	0.000	0
1	0.017	68.483	0.133	0.028	3.611	42.819	0.028	68.370	0.114	0
2	0.035	136.946	0.134	0.056	3.582	85.257	0.056	136.865	0.081	-6.9E-17
3	0.052	205.366	0.134	0.084	3.552	127.293	0.084	205.394	-0.028	0
4	0.070	273.724	0.135	0.112	3.523	168.911	0.112	273.885	-0.161	-1.8E-16
5	0.087	341.999	0.136	0.141	3.493	210.094	0.141	342.280	-0.281	0
10	0.175	681.395	0.139	0.286	3.341	410.777	0.286	684.346	-2.950	0
15	0.262	1015.606	0.142	0.435	3.185	598.857	0.435	1019.987	-4.381	0
20	0.349	1342.087	0.145	0.587	3.024	773.447	0.587	1348.077	-5.989	0
25	0.436	1658.354	0.149	0.743	2.859	933.563	0.743	1666.798	-8.443	0
30	0.524	1962.000	0.153	0.902	2.688	1078.054	0.902	1973.133	-11.133	0
35	0.611	2250.714	0.156	1.066	2.511	1205.635	1.066	2263.463	-12.749	0
40	0.698	2522.299	0.161	1.234	2.328	1314.942	1.234	2534.573	-12.274	0
45	0.785	2774.687	0.165	1.407	2.137	1404.541	1.407	2784.479	-9.792	0
50	0.873	3005.958	0.170	1.586	1.936	1472.868	1.586	3012.587	-6.628	0
55	0.960	3214.353	0.177	1.771	1.723	1518.103	1.771	3218.850	-4.498	0
60	1.047	3398.284	0.184	1.964	1.492	1538.026	1.964	3401.883	-3.599	0
65	1.134	3556.352	0.194	2.167	1.236	1530.108	2.167	3556.514	-0.162	0
70	1.222	3687.354	0.205	2.382	0.936	1492.786	2.382	3673.616	13.738	0
75	1.309	3790.293	0.219	2.610	0.534	1435.961	2.610	3765.149	25.144	0

This verification was done by putting $R(\theta)$ from (25) into (14) and comparing it with the displacement of cable (L_1). The comparison is shown in Table 2-7 as (L_{cw}-L_{cable}). We observed that these differences tend to zero, so the polynomial form of $R(\theta)$ is acceptable.

Also, T_{cable} was calculated by using equation (11), and we compared it with T_{CW} as shown in Table 2-7 as (T_{cw}-T_{cable1}). We observed that the maximum torque difference was 25 Nm. The percentage error was 1%.

2.3.6. Cam Profile Completion:

1. The cam profile was described by equation (25), so we could get the cam profile from 0° to 90°. We could not apply the same equation to a 360° profile, since at some point the cam radius diminishes to zero and then becomes negative.

2. To complete the profile, we divided the cam profile equation into two parts, where the first part was spanning 0 to 75° would satisfy equation (25) and from 75° to 360° we would develop a new equation.

3. The transition point was chosen as 75° by an iterative method considering the resultant profile and the difference in torque values. For a transition point at 90°, the resultant cam profile was too big.

    a) The new equation was a 3rd-degree polynomial, denoted as

    $$R_2(t) = a\theta^3 + b\theta^2 + c\theta + d \qquad (26)$$

    b) For continuity of the profile, the value $R(\theta)$ and slope $\dfrac{dR}{d\theta}$ of (25) and (26) at points

        $\theta = 75°$ and $\theta = 0°/360°$ should be equal.

    c) Therefore, we got four equations and four variables to solve:

    $$\begin{aligned}
    R_2(t) &= a\theta + b\theta^2 + c\theta + d = 0.2185 \\
    R_2(t) &= a\theta + b\theta^2 + c\theta + d = 0.1323 \\
    \frac{dR_2(t)}{d\theta} &= a\theta^2 + b\theta + c\theta = 0.1648 \\
    \frac{dR_2(t)}{d\theta} &= a\theta^2 + b\theta^2 + c\theta = 0.0447
    \end{aligned} \qquad (27)$$

    d) Solving equation (27), we got

    $$R_2(t) = 0.009871\theta^3 - 0.124490\theta^2 + 0.440030\theta - 0.16633 \qquad (28)$$

4. The resultant cam profile is shown in Figure 2-9 and is given by equation (25) for 0°

to 75° and equation (28) for 75° to 360°.
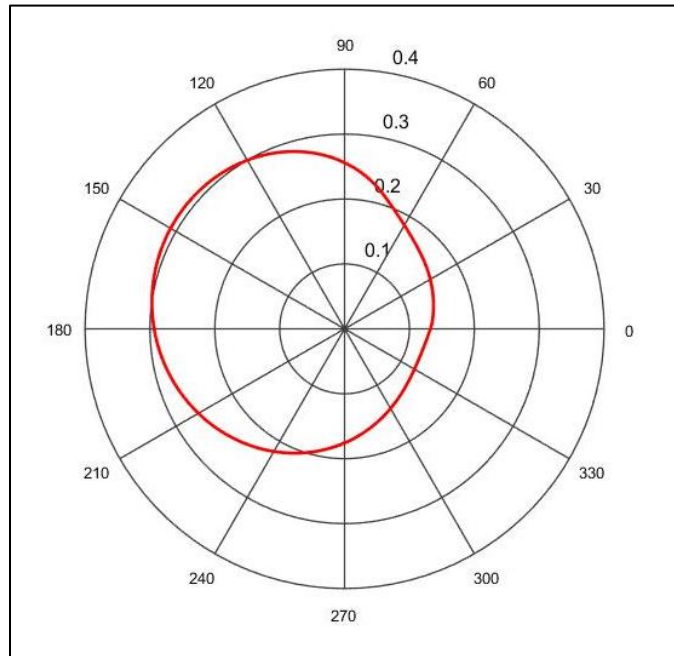
Figure 2-9 Cam profile (units of degrees and meters)

2.4. Effect of Change in Payload Position

The cam design was done for a reference height of two meters. In most cases, we intended to keep the same reference height. But we needed to know the effect of the change in payload position on torque requirements and balancing of payload. The following analysis was done for an increase and decrease in payload position by 0.3m.

2.4.1. Decrease in Payload Position

For a decrease in payload height by 0.3 m, that is $y = 1.35$ m, we calculated design parameters as described in section 2.3.

Table 2-8. Effect of decrease in payload height ($y = 1.35$ m) for same design parameters

Sr No.	Theta	T_{CW}	$R(\theta)$	L_{cam}	X	L_1	T_{cable1}	T_{cw}-T_{cable}	L_{cw}-L_{cable}
0	0.000	0.000	0.132	0.000	3.640	0.000	0.000	0.000	0
1	0.017	68.483	0.133	0.028	3.610	0.028	55.865	12.619	-4.545E-16
2	0.035	136.946	0.134	0.056	3.580	0.056	111.874	25.072	-6.939E-17
3	0.052	205.366	0.134	0.084	3.550	0.084	167.955	37.412	0
4	0.070	273.724	0.135	0.112	3.520	0.112	224.049	49.675	-1.804E-16
5	0.087	341.999	0.136	0.141	3.489	0.141	280.110	61.889	0
10	0.175	681.395	0.139	0.286	3.333	0.286	561.254	120.141	0
15	0.262	1015.606	0.142	0.435	3.172	0.435	838.541	177.065	0
20	0.349	1342.087	0.145	0.587	3.006	0.587	1111.276	230.811	0
25	0.436	1658.354	0.149	0.743	2.835	0.743	1378.253	280.101	0
30	0.524	1962.000	0.153	0.902	2.657	0.902	1637.342	324.658	0
35	0.611	2250.714	0.156	1.066	2.471	1.066	1886.004	364.710	0
40	0.698	2522.299	0.161	1.234	2.278	1.234	2122.171	400.128	0
45	0.785	2774.687	0.165	1.407	2.074	1.407	2345.053	429.634	0
50	0.873	3005.958	0.170	1.586	1.858	1.586	2555.503	450.456	0
55	0.960	3214.353	0.177	1.771	1.623	1.771	2755.812	458.541	0
60	1.047	3398.284	0.184	1.964	1.363	1.964	2949.311	448.972	0
65	1.134	3556.352	0.194	2.167	1.058	2.167	3142.111	414.240	0
70	1.222	3687.354	0.205	2.382	0.655	2.382	3364.558	322.796	0

1. We got a maximum difference in torque requirement of 458 Nm as shown in column "T_{cw}-T_{cable}" of Table 2-8 for a payload of 150 kg and counterweight of 400 kg. We got a difference in cable length wrapping on the cam from the displacement of cable length in the workspace approximately equal to zero.

2. If we changed the counterweight to 355 kg, we got the difference in torque requirements as 117 Nm. This torque requirement for this set of boundary conditions at various positions and theta values are shown in Table 2-9

3. For a payload height of ($y = 1.25$ m) and a counterweight of $W_{cw} = 365$ kg, we got the maximum difference in torque requirement as 70 Nm.

Table 2-9. Torque Requirement for Payload at $y = 1.35$m and Counterweight $W_{cw} = 475$ kg

Sr No.	Theta	T_{CW}	X	T_{cable1}	$T_{cw}-T_{cable}$
0	0.000	0.000	3.640	0.000	0.000
1	0.017	60.779	3.610	55.865	4.914
2	0.035	121.539	3.580	111.874	9.666
3	0.052	182.263	3.550	167.955	14.308
4	0.070	242.930	3.520	224.049	18.881
5	0.087	303.524	3.489	280.110	23.414
10	0.175	604.738	3.333	561.254	43.484
15	0.262	901.350	3.172	838.541	62.809
20	0.349	1191.102	3.006	1111.276	79.826
25	0.436	1471.789	2.835	1378.253	93.537
30	0.524	1741.275	2.657	1637.342	103.933
35	0.611	1997.509	2.471	1886.004	111.505
40	0.698	2238.540	2.278	2122.171	116.369
45	0.785	2462.535	2.074	2345.053	117.482
50	0.873	2667.788	1.858	2555.503	112.285
55	0.960	2852.738	1.623	2755.812	96.926
60	1.047	3015.977	1.363	2949.311	66.665
65	1.134	3156.262	1.058	3142.111	14.151
70	1.222	3272.527	0.655	3364.558	-92.031

4.   Since the positions at which these differences occur varies due to the complex nature of the equations, we could not develop a relation between payload and counterweight. We needed to rely on Excel calculations to determine the counterweight. For example, for conditions of $y = 1.25$ m and $Wcw = 365$ kg, the maximum torque requirement occurs at $x = 2.29$m, while for $y = 1.35$ m and $Wcw = 365$ kg, it occurs at $x = 2.07$ m.

2.4.2.Increase in Payload Position

For an increase in payload height by 0.3 m, that is $y = 0.75$ m, we calculated design parameters as described in section 2.3.

Table 2-10. Effect of increase in payload height (y = 0.75 m) for same design parameters

Sr No.	Theta	T_{CW}	$R(\theta)$	L_{cam}	X	L_1	T_{cable1}	T_{cw}-T_{cable}	L_{cw}-L_{cable}
0	0.000	0.000	0.132	0.000	3.640	0.000	0.000	0.000	0
1	0.017	68.483	0.133	0.028	3.612	0.028	92.089	-23.606	0
2	0.035	136.946	0.134	0.056	3.583	0.056	184.292	-47.347	-6.939E-17
3	0.052	205.366	0.134	0.084	3.554	0.084	276.486	-71.119	0
4	0.070	273.724	0.135	0.112	3.525	0.112	368.569	-94.844	-1.804E-16
5	0.087	341.999	0.136	0.141	3.496	0.141	460.461	-118.462	0
10	0.175	681.395	0.139	0.286	3.347	0.286	919.067	-237.672	0
15	0.262	1015.606	0.142	0.435	3.195	0.435	1367.224	-351.618	0
20	0.349	1342.087	0.145	0.587	3.038	0.587	1803.139	-461.052	0
25	0.436	1658.354	0.149	0.743	2.878	0.743	2224.037	-565.683	0
30	0.524	1962.000	0.153	0.902	2.712	0.902	2625.464	-663.464	0
35	0.611	2250.714	0.156	1.066	2.542	1.066	3002.078	-751.365	0
40	0.698	2522.299	0.161	1.234	2.366	1.234	3348.951	-826.653	0
45	0.785	2774.687	0.165	1.407	2.184	1.407	3662.559	-887.872	0
50	0.873	3005.958	0.170	1.586	1.994	1.586	3940.790	-934.832	0
55	0.960	3214.353	0.177	1.771	1.795	1.771	4181.459	-967.107	0
60	1.047	3398.284	0.184	1.964	1.584	1.964	4379.097	-980.813	0
65	1.134	3556.352	0.194	2.167	1.356	2.167	4520.072	-963.720	0
70	1.222	3687.354	0.205	2.382	1.104	2.382	4576.851	-889.497	0
75	1.309	3790.293	0.219	2.610	0.813	2.610	4504.815	-714.522	0
80	1.396	3864.386	0.232	2.854	0.427	2.854	4245.665	-381.279	0

1.   We got a maximum difference in torque requirement of 980 Nm as shown in column "*Tcw-Tcable*" of Table 2-10. We got a difference in the cable length wrapping on the cam from the displacement of cable length in the workspace approximately equal to zero.

2.   If we changed the counterweight to 475 kg, we got the difference in torque requirements as 371 Nm. The torque requirement for this set of boundary conditions at various positions and theta are shown in Table 2-11.

3.   For a payload height of (y = 0.85 m) and counterweight of W_{cw} = 465 kg, we got the

maximum difference in torque requirement as 75 Nm.

Table 2-11. Torque requirement for payload at y =0.75m and counterweight W_{cw} = 475 kg

Sr No.	Theta	T_{CW}	X	T_{cable1}	T_{cw}-T_{cable}
0	0.000	0.000	3.640	0.000	0.000
1	0.017	81.324	3.612	92.089	-10.765
2	0.035	162.623	3.583	184.292	-21.669
3	0.052	243.872	3.554	276.486	-32.613
4	0.070	325.048	3.525	368.569	-43.521
5	0.087	406.124	3.496	460.461	-54.337
10	0.175	809.157	3.347	919.067	-109.910
15	0.262	1206.032	3.195	1367.224	-161.191
20	0.349	1593.728	3.038	1803.139	-209.411
25	0.436	1969.295	2.878	2224.037	-254.741
30	0.524	2329.875	2.712	2625.464	-295.589
35	0.611	2672.723	2.542	3002.078	-329.356
40	0.698	2995.230	2.366	3348.951	-353.722
45	0.785	3294.941	2.184	3662.559	-367.619
50	0.873	3569.576	1.994	3940.790	-371.215
55	0.960	3817.044	1.795	4181.459	-364.416
60	1.047	4035.462	1.584	4379.097	-343.635
65	1.134	4223.168	1.356	4520.072	-296.904
70	1.222	4378.733	1.104	4576.851	-198.118
75	1.309	4500.973	0.813	4504.815	-3.842
80	1.396	4588.958	0.427	4245.665	343.293

2.4.3. Summary of changes in payload position

It was difficult to track the torque requirement at various positions, but we

concluded that as payload height increased the variation in torque requirement

increased, and we needed to increase the counterweight, so as to require less

compensatory motor torque.

Chapter 3 - Design of Components

In chapter 2, we derived a cam profile to balance a load vertically while maintaining zero net force on the payload horizontally.

The partial body weight offload system comprised a cam (non-circular spool), gear box, spools, counterweight arm, cam shaft, and rope and pulley system as shown in Figure 2-1.

The components were designed by considering the system as static.

As discussed in the previous chapter, the cam was designed for the parameters shown in Table 3-1. Therefore, for designing the rest of the components, we used design parameters from Table 2-1 and loads and torque values from Table 2-7.

Table 3-1. Design parameters after cam design

Parameters	Value
Payload (W_P)	152 kg
Payload Height from Top (H_P) (Reference Height)	1.05 m
Length of Counterweight Arm (L_{CW})	1 m
Gear Box Ratio (κ)	12
Counterweight (W_{CW})	400 kg
Maximum Tension in the Rope (refer to Table 2-7.)	1530 N
Maximum Torque at Counterweight Arm (refer to Table 2-7.)	3790.293 Nm

3.1. Gear Box Design

The gear box comprises gears and circular spools. The layout of the gear box is as shown in Figure 3-1.
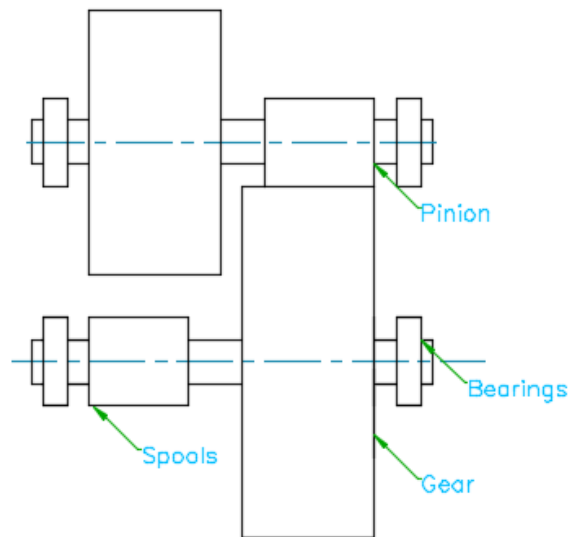

Figure 3-1 Gear Box Layout

3.1.1. Selection of the Gear Box Ratio:

The gear box ratio was calculated from equation (22), as

$$\kappa \geq \frac{\sqrt{L^2 + (y-e)^2} - (y-e)}{\int_0^{\pi/2} R d\theta} \tag{22}$$

Here,

$L = 3.65$ m

$(y\text{-}e) = 1.05$ m

$\int_0^{\pi/2} R d\theta = 0.277$

Substituting the above values gave $\kappa \geq 9.91$. Therefore, the selected gear box

ratio is 12, rounding up to the nearest highly factorable integer.

Since the gear box ratio is 12, and 10 is an upper bound on the reduction ratio for

a single gear stage, we needed to arrange a combination of gears and spools to 12. Factors

of 12 are either 6 and 2, or 4 and 3. Therefore, gears with a ratio of 4 and spools with the

size ratio of 3 were selected for design of the gear box.

The larger spool and smaller gear (pinion) were installed on the one shaft denoted

as shaft-1 for calculations. The smaller spool and larger gear were installed on the other

shaft denoted as shaft-2. The rope from the payload went through a pulley and was

wound on the larger spool. The nylon strap was wound on the smaller spool and then was

wound on the cam. The tension in the rope revolved the larger spool and was balanced by

the cam system design in chapter 2.

3.1.2. Gear Shaft Design for Stresses:

The shaft material was 1045 carbon steel (McMaster-Carr). Properties were:

Yield Strength – 75,000 psi (510 MPa)

Young's Modulus – 29,000 ksi (210 GPa)

We designed for shafts loading in which the bending moment contributes most

heavily to stress [28]. The free body diagrams are shown in Figure 3-2 and Figure 3-5,

with associated shear and moment diagrams in Figures 3-3, 3-4, 3-6, and 3-7.

a. Stress Analysis in Shaft-1.

The larger spool and pinion (smaller gear) were installed on Shaft-1. Forces

coming from the payload were considered for the design of this shaft.

Figure 3-2 Free body diagram of shaft 1

The reactions were calculated as:

$$\sum F = 0. \quad \Longrightarrow \quad R_A + R_B + 1538 - 4614 = 0. \tag{29}$$

$$\sum M = 0. \quad \Longrightarrow \quad 57.975 \times 1538 - 153.195 \times 4614 + 204.7875 R_B = 0 \tag{30}$$

This gives $R_A = 59.6N$ and $R_B = 3016.4N$.

The bending moment and shear force diagrams for shaft 1 are as shown below.

Figure 3-3 Shear force diagram for shaft 1

Figure 3-4 Bending moment diagram for shaft 1

The maximum bending moment is 155.624 Nm and the maximum shear force is 3016 N.

Bending stress in the shaft is given by Hearn [29]:

$$\sigma_b = \frac{My}{I} \qquad (31)$$

Here, $y = d/2$

and
$$I = \frac{\pi d^4}{64} \qquad (32)$$

Therefore,
$$\sigma_b = \frac{32M}{\pi d^3} \qquad (33)$$

Allowable bending stress is

$$\sigma_b = \frac{S_y}{SF} = \frac{510}{1.5} = 340 MPa \qquad (34)$$

where *SF* is a factor of safety, considered as 1.5.

Therefore, the minimum diameter is

$$d = \sqrt[3]{\frac{32M}{\sigma_b \times \pi}} = \sqrt[3]{\frac{32 \times 155.6 \times 1000}{340 \times \pi}} = 16.7mm \qquad (35)$$

b. Stress Analysis in Shaft-2.

A smaller spool and a larger gear were installed on Shaft-2. Forces coming from the counterweight were considered for the design of this shaft.
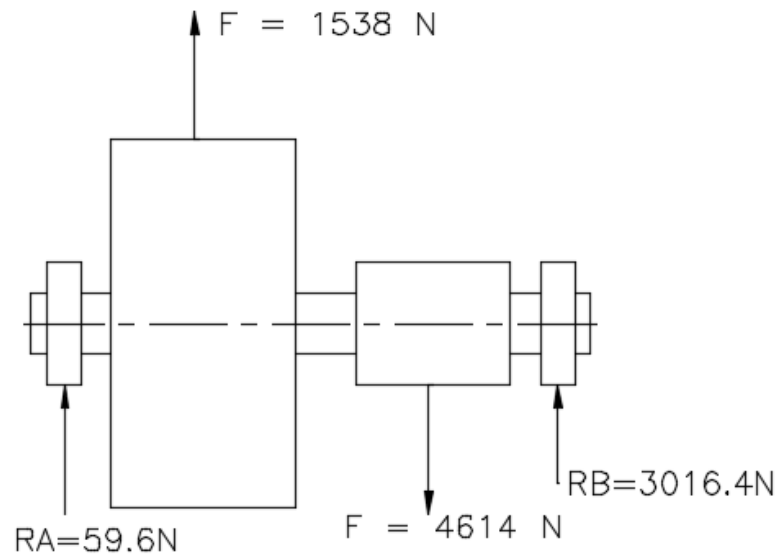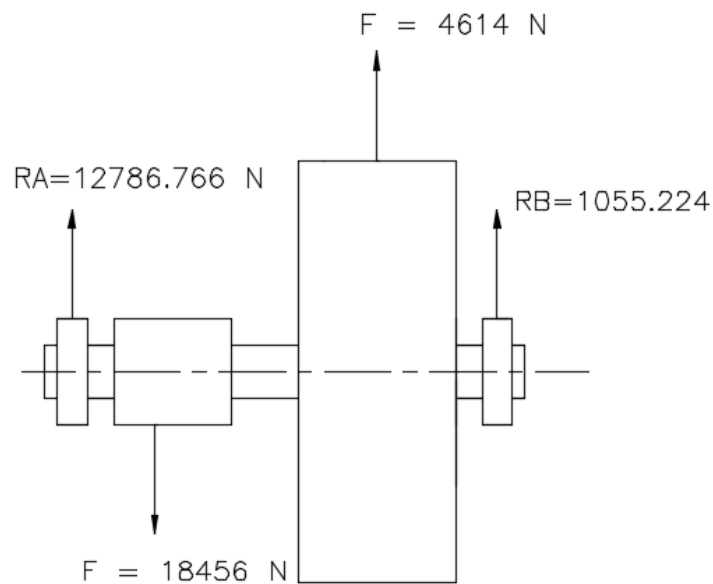

Figure 3-5 Free body Diagram of Shaft 2

The reactions are calculated as:

$\sum F = 0.$ ⟹ $R_A + R_B + 18456 - 4614 = 0.$ (36)

$\sum M = 0.$ ⟹ $57.975 \times 18456 - 153.195 \times 4614 + 204.7875 R_B = 0$ (37)

This gives $R_A = -12786.76N$ and $R_B = -1055.2N$.

The bending moment and shear force diagrams for shaft 2 are as shown below.

Figure 3-6 Shear force diagram for shaft 2
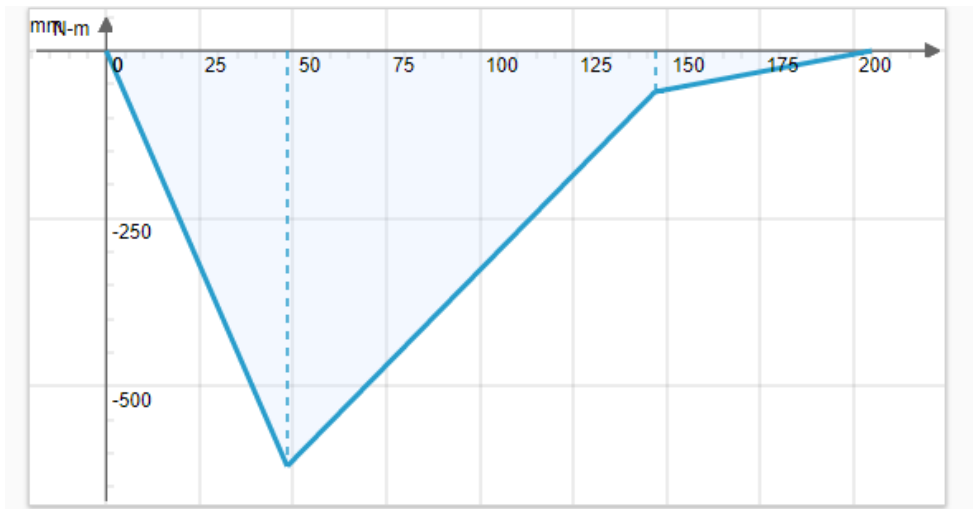
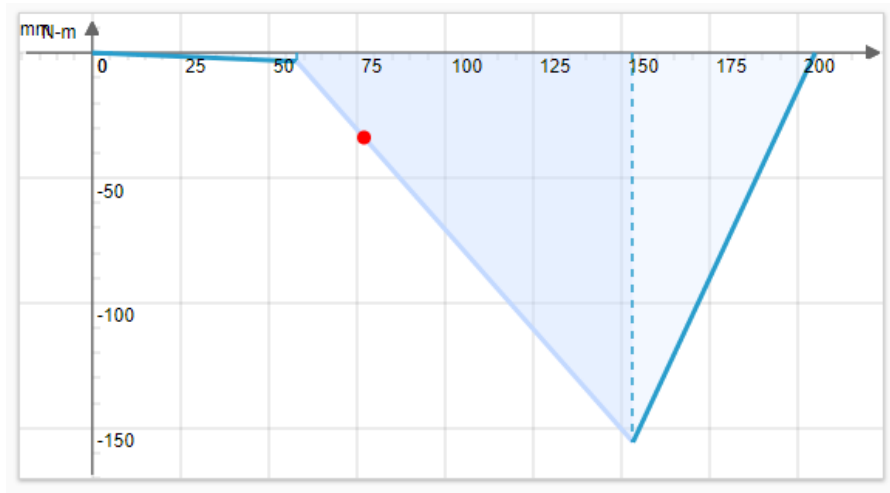*Figure 3-7 Bending moment diagram for shaft 2*

Using the same equation (35) as above for allowable stress, the minimum diameter is

$$d = \sqrt[3]{\frac{32M}{\sigma_b \times \pi}} = \sqrt[3]{\frac{32 \times 619 \times 1000}{340 \times \pi}} = 26.47mm \qquad (38)$$

3.1.3. Selection of gears.

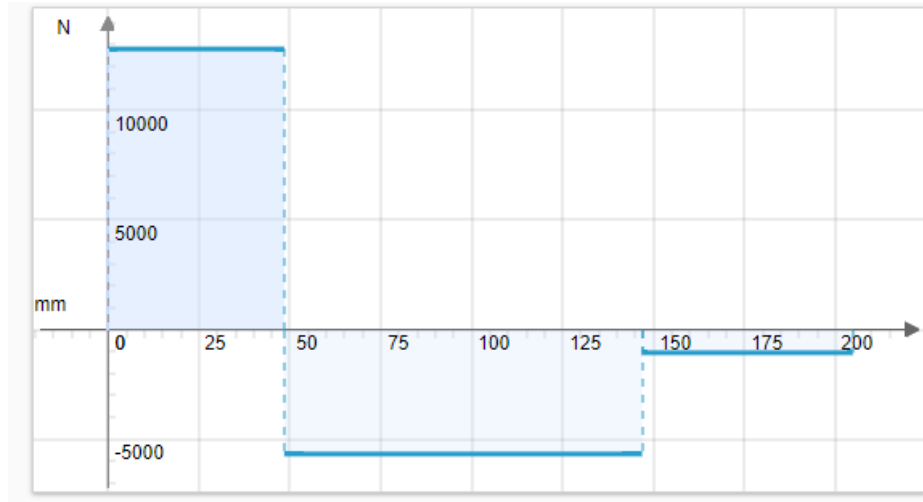The Lewis form factor bending stress ($\sigma^g{}_b$) in gears is given by Budynas, Nisbett, and Shigley [28]:

$$\sigma^g{}_b = \frac{W^t}{F_w p y} = \frac{W^t}{F_w Y m} \tag{39}$$

where

- W^t – Transmitted load = 4614 N

- F_w – Net face width of gear

- p - Circular pitch

- m - module = 4 mm

- y, Y – Lewis form factor, $Y = 0.296$

- Material of procured gear supplier i.e. Boston Gear is Mild Carbon Steel which has

yield strength of $Sy = 440$MPa.

- Allowable bending stress is

$$\sigma^g{}_b = \frac{S_y}{SF} = \frac{440}{1.5} = 293 \tag{40}$$

Therefore,

$$293 = \frac{4614}{F_w \times 0.296 \times 4} \tag{41}$$

$F_w = 13.3$ mm is the minimum face width.

For the final selection of gears refer to Table 3-2.

Table 3-2. Gear selection parameters

	Gear		**Pinion**	
No. of Teeth	64	64	16	16
Pressure Angle	20°			
Pitch Diameter	256 mm	8 inch	64 mm	2 inch
Face Width	15 mm	0.75inch	15 mm	0.75 inch
Module	4 mm		4 mm	
Diametrical Pitch		6.35		6.35
Bore	27 mm	1 1/8"	25 mm	1"

We selected a gear from the Boston catalog as shown in Appendix B-1.

Note: For testing of the prototype, gears and bearings were selected with a bore of one inch diameter.

3.1.4. Failure Analysis of Key:

For 1" & 1.125" bores, the standard key available is ¼" x ¼".

Maximum torque in the system is

$$T_{\max} = F \times d_{spool} = 4150 \times 2 \tag{42}$$

$$T_{\max} = 8300 \text{lb-inch} \tag{43}$$

Shear force is given by

$$F_S = \frac{2 T_{\max}}{d} = 14755 \text{lb} \tag{44}$$

Shear stress in the key is

$$\tau = \frac{F_S}{L_k b_k} \tag{45}$$

Maximum shear stress for steel (Shear Stress Failure Theory [28]) is

$$\tau = \frac{S_y}{2} = 37500 \text{psi} \tag{46}$$

Allowable shear stress is

$$\tau_{allow} = \frac{\tau}{SF} = \frac{37500}{1.5} = 25000\text{psi} \tag{47}$$

Therefore, from equations (44), (45) and (47),

$$L_k = 2.3 \text{ in.} \tag{48}$$

Note: For testing, we considered 2" width of smaller spool and length of key since pilot testing will not be at maximum load.

3.1.5. Spool Design

Rope from the payload wound on the larger spool. The size difference between the larger and smaller spool was three times. If the smaller spool is chosen to be two inches in diameter, the larger spool is six inches in diameter.

Width of the larger spool is calculated as

$$6\pi(\frac{W_{spool}}{0.3937}) = L_{cable} \tag{49}$$

Here, 0.3937 inch is the nominal rope diameter.

From equation 15, with x = 0,

$$L_{Cable} = \sqrt{144^2 + 30^2} - 30 = 117.1 \text{ in}$$

By Equation (41)

$$6\pi W_{spool} = 85.138 \times 0.3937; \tag{50}$$

$$W_{spool} = 2.44 \approx 3\text{in} \tag{51}$$

The width of the smaller spool was equal to the width of the strap which was two inches.

3.1.6. Gear Box Housing Design:

The gear box was mounted on a wooden vertical post, as shown in Figure 3-8. The main challenge with this assembly was to design bolts for failure in shear. There were also complex reaction forces coming on the gearbox housing.

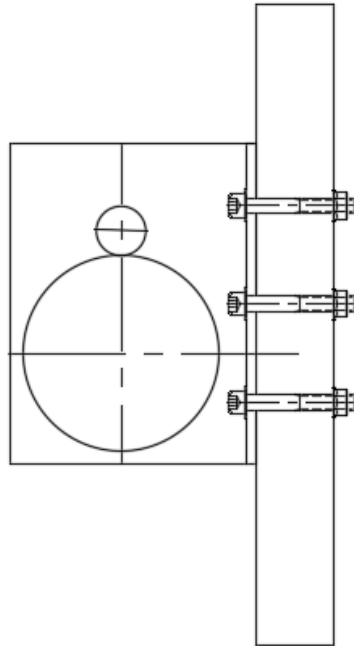*Figure 3-8 Gear box mounted on vertical post*

We selected the gear box housing to be made up of ⅜" steel plate.

The approximate bolt diameter is given by

$$d_{fb} \geq \sqrt[3]{2T_{max}} \tag{52}$$

Here, $T_{max} \approx 1000$ Nm.

$$d_{fb} \geq (2T_{max})^{\frac{1}{3}} = 0.5" \tag{53}$$

Therefore, we selected the bolt diameter as 9/16".

Calculations for shear stress in the bolt are given by

$$\tau = \frac{F}{Na} \qquad (54)$$

The shear stress area of a 9/16-18 grade bolt is $a = 0.2030$ in^2

$$F = 18456 + 1538, \ N = 4496 \text{ lb}, \qquad (55)$$

Number of bolts: $N = 6$.

Therefore, shear stress in the bolt is

$$\tau = \frac{4496}{6 \times 0.2030} = 14765 psi \qquad (56)$$

3.2. Cam Shaft

Bending stresses in the cam shaft were neglected due to the very short length of the shaft.

Shear stress in torsion is given by

$$\tau = \frac{Tr}{J} = \frac{16T}{\pi d^3} \qquad (57)$$

Here T is the total torque applied on the cam shaft and is given by

$$T = T_1 \ \text{or} \ T_2 \qquad (58)$$

where

$T_1 = 4000$ Nm (torque due to the counterweight)

or $T_2 = 4000$ Nm (torque due to the payload or tension in the strap).

The maximum shear stress for steel (Shear Stress Failure Theory [28]) is

$$\tau = \frac{S_y}{2} = 255Nm \qquad (59)$$

The allowable shear stress is

$$\tau_{allow} = \frac{\tau}{SF} = \frac{255}{1.5} = 170 Nm \qquad (60)$$

Therefore,

$$d = \sqrt[3]{\frac{16 \times 4000 \times 1000}{\pi \times 170}} = 30.58 mm \qquad (61)$$

Therefore, the cam shaft, d = 1.25" (31.75mm).

3.2.1. Failure Analysis of Key:

For the 1.125" bore, the standard key available is ¼" x ¼".

The maximum counterweight of the system was 4000 N and the length of the counterweight arm was 1 m. Therefore, the maximum torque in the cam shaft was

$$T = 8450 \text{ lb-in (954.75 Nm).} \qquad (62)$$

Shear force is given by

$$F_S = \frac{2T}{d} = 13520 lb \qquad (63)$$

Shear stress in the key is

$$\tau = \frac{F_S}{Lb} \qquad (64)$$

Maximum shear stress for steel (Shear Stress Failure Theory [28]) is

$$\tau = \frac{S_y}{2} = 375000 psi \qquad (65)$$

Allowable shear stress is

$$\tau_{allow} = \frac{\tau}{SF} = \frac{37500}{1.5} = 25000 psi \qquad (66)$$

Therefore,

$$L = \frac{13520}{25000 \times 0.25} \qquad (67)$$

$L = 2.16$ in.

Therefore, we selected a shaft size of 1.25" diameter, with the corresponding key of

reasonable length to match the cam thickness.

3.3. Counterweight Arm
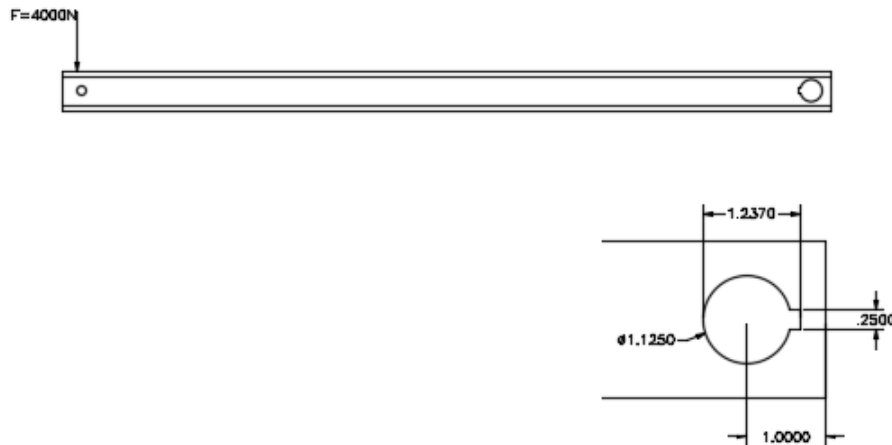
Figure 3-9 Counterweight arm layout

The counterweight arm is the square bar keyed to the cam shaft. Since torque in

the cam shaft is equal to that of the counterweight arm, the dimension of the

counterweight arm width was 2.5" x 2.5", equal to the key length as calculated in section

3.2.1. The bore in the counterweight arm acts as a slotted beam, with stresses in the

slotted beam given as,

$$\sigma_{allow} = \frac{M_A}{I / c} \qquad (68)$$

where *I/c* is the section modulus of the cross section of the weakest part of the slotted

beam [30].

Allowable bending stress is

$$\sigma_{allow} = \frac{Sy}{SF} = \frac{510}{1.5} = 340 MPa \tag{69}$$

$$I \approx \frac{h^2 wt}{2} \tag{70}$$

$h = w = 2.5$" (width of counterweight arm)

$$t_{cw} = \frac{h-d}{2} = .375" \tag{71}$$

$w = h = 2.5$"

$F = 4,000 \text{ N} \approx 900 \text{ lb.}$

$L_{cw} = 1000 \text{ mm} = 39.37 \text{ in.}$

E (steel) = 210 GPa = 210 x 10^3 MPa

$$\sigma_{max} = \frac{FL_{cw}}{hwt_{cw}} = \frac{1000 \times 39.37}{2.5 \times 2.5 \times 0.375} = 15118 psi \tag{72}$$

Therefore,

$$SF = \frac{50000}{15118} = 3.3 \tag{73}$$

 Therefore, a counterweight arm of 2.5" x 2.5" of 37.39" length was acceptable.

3.4.   Dynamic Analysis

Consider the counterweight rotating through the counterweight arm of length, 1m,

at a constant angular velocity of ω_1. Let the mass of the counterweight be m_{cw}.

Therefore, the velocity of the counterweight is given by [31, 32]

$$v_{cw} = \dot{r}_{cw} = \dot{r}\,e_r + r\dot{\theta}\,e_\theta = L_{cw}\omega e_\theta \qquad (74)$$

since , $\dot{r} = 0$, $\dot{\theta} = \omega$ and $r = L_{cw}$.
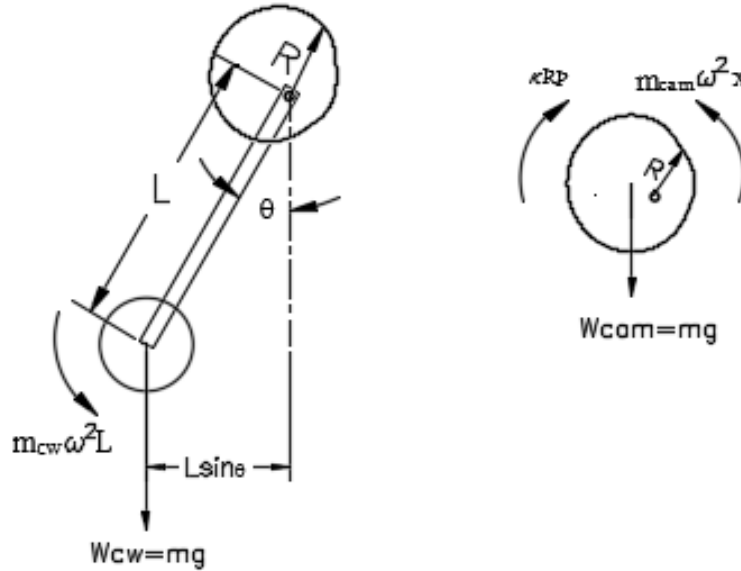
Figure 3-10 Free body diagram for counterweight-cam system

Acceleration of the counterweight is

$$a_{cw} = \ddot{r}_{cw} = (\ddot{r} - r\dot{\theta}^2)e_r + (r\ddot{\theta} + 2\dot{r}\dot{\theta})e_\theta \qquad (75)$$

Here, $\dot{r} = 0$ $\ddot{r} = 0, \dot{\theta} = \omega_1$, $\ddot{\theta} = \omega_1$ and $r = L_{cw}$. Therefore,

$$a_{cw} = L_{cw}\omega^2 e_r + L_{cw}\dot{\omega}e_\theta \qquad (76)$$

Assuming zero friction in the counterweight shaft,

$$\sum F = m\ddot{r} \qquad (77)$$

$$F_1 = m_{cw}L_{cw}\omega^2 e_r + m_{cw}L_{cw}\dot{\omega}e_\theta + m_{cw}g e_y \qquad (78)$$

where, F_1 is a net force on the counterweight system that is carried by reaction loads at the shaft.

Moments about the cam shaft can be given as,

$$\sum M = \sum r \times F \tag{79}$$

$$\sum M_1 = re_r \times (m_{cw}L_{cw}\omega^2 e_r + m_{cw}L_{cw}\dot{\omega}e_\theta + m_{cw}ge_y) \tag{80}$$

$$\sum M_1 = (m_{cw}L_{cw}^2\dot{\omega}e_z + m_{cw}gL_{cw}\sin\theta e_z) \tag{81}$$

$$\sum M_1 = (I_{cw}\dot{\omega} + m_{cw}gL\sin\theta)e_z \tag{82}$$

It is observed that, in (82), the second term represents the torque (T_{cw}) applied at the center of the cam due to the counterweight, while the first term represents the torque ($T_{cw\_inertia}$) due to the effect of the inertia of the counterweight on the system. This inertia effect depends on the angular acceleration of the counterweight.

Taking the ratio of $T_{cw\_inertia}$ and T_{cw} from (81),

$$\frac{T_{cw\_Inertia}}{T_{cw}} = \frac{\dot{\omega}L_{cw}}{g} \tag{83}$$

To have minimum effect of counterweight inertia, ratio (83) should be less than 10%. Therefore,

$$\frac{\dot{\omega}L}{g} \leq 0.1 \tag{84}$$

For $L_{cw} = 1$m and $g \approx 10$m/s².

$$\dot{\omega} \leq 1 \quad \text{rad/s}^2 \tag{85}$$

The average cam radius was 0.2 m and gear box ratio κ was 12; to have the effect of inertia under 10%, maximum acceleration (or deacceleration) of payload should not be more than,

$$a_p \leq 2.4\,\text{m/s}^2 \tag{86}$$

Acceleration of the cam is given by (76),

From equation (25),

$$R(\theta) = -0.0708\theta^6 + 0.2856\theta^5 - 0.404\theta^4 + 0.2702\theta^3 - 0.078\theta^2 + 0.0447\theta + 0.1323$$

We can rewrite $\dot{r}$ as,

$$\dot{r} = \frac{dr}{d\theta}\dot{\theta} \tag{87}$$

Therefore,

$$\dot{r} = (-0.4248\theta^5 + 1.428\theta^4 - 1.616\theta^3 + 0.8106\theta^2 - 0.156\theta + 0.0447)\omega_2 \tag{88}$$

where $\dot{\theta} = \omega$ is the angular velocity of the cam.

We can also write $\ddot{r}$ as

$$\ddot{r} = \frac{d}{dt}\dot{r} \tag{89}$$

$$\ddot{r} = (-2.124\theta^4 + 5.712\theta^3 - .4.848\theta^2 + 16212\theta - 0.156)\omega_2^2 +$$
$$(-0.4248\theta^5 + 1.428\theta^4 - 1.616\theta^3 + 0.8106\theta^2 - 0.156\theta + 0.0447)\dot{\omega}_2 \tag{90}$$

Since, $\ddot{\theta} = \dot{\omega}$. Therefore,

$$\ddot{r} = (-2.124\theta^4 + 5.712\theta^3 - .4.848\theta^2 + 16212\theta - 0.156)\omega_2^2 \tag{91}$$

Therefore by (68),

$$a_{cam} = \ddot{r}_{cam} = ((-2.124\theta^4 + 5.712\theta^3 - .4.848\theta^2 + 16212\theta - 0.156)\omega^2 -$$
$$(-0.0708\theta^6 + 0.2856\theta^5 - 0.404\theta^4 + 0.2702\theta^3 - 0.078\theta^2 + 0.0447\theta + 0.1323)\omega^2)e_r \quad (92)$$
$$+ ((-0.0708\theta^6 + 0.2856\theta^5 - 0.404\theta^4 + 0.2702\theta^3 - 0.078\theta^2 + 0.0447\theta + 0.1323)\dot{\omega}$$
$$2(-0.4248\theta^5 + 1.428\theta^4 - 1.616\theta^3 + 0.8106\theta^2 - 0.156\theta + 0.0447)\omega^2)e_\theta$$

Summing forces,

$$\sum F_2 = F_S + F_{cam} + W_{cam} = F_2 \quad (93)$$

where F_S is the force in the strap, F_{cam} is the inertial force acting on the cam due to a_{cam} given by (89), W_{cam} is the weight of the cam, and F_2 is the net force on the cam.

$$F_{cam} = m_{cam}a_{cam} = m_{cam}((\frac{d^2R}{d\theta^2} - R)\omega^2 e_r + (R\dot{\omega}_2 + 2\frac{dR}{d\theta}\omega^2)e_\theta) \quad (94)$$

$$W_{cam} = m_{cam}ge_y \quad (95)$$

The mass of the manufactured cam profile (refer to section 4.1 for manufacturing details) is,

$$m_{cam} = (3 \times 2.665 + 2 \times 1.769) = 11.533\text{kg} \quad (96)$$

$$W_{cam} = 113N \quad (97)$$

Balancing the moments,

$$\sum M_2 = \sum r \times F \quad (98)$$

$$\sum M_2 = re_r \times (F_S + F_{cam} + W_{cam}) \quad (99)$$

$$\sum M_2 = (F_S R + (R^2\dot{\omega} + 2R\frac{dR}{d\theta}\omega^2)m_{cam} + m_{cam}gc)e_z \quad (100)$$

In (100), the first term $F_S R$ is tension in the strap due to the payload. The second term is the effect of inertia of the cam. This effect depends on two terms; first, the inertia effect due to angular acceleration of the cam, and second, the inertia effect due to the non-

circularity of the cam. This effect was not considered in static balancing. The third term comes out to be the effect of the unbalanced cam on the system. Term "c" in (100) is the distance between center of gravity of the cam and the axis of rotation. We can minimize this effect by the balancing of the cam.

From the profile of the cam (refer to Figure 3-11), the center of gravity is located at points (-82.63 mm, 40.01 mm) from the axis of rotation.

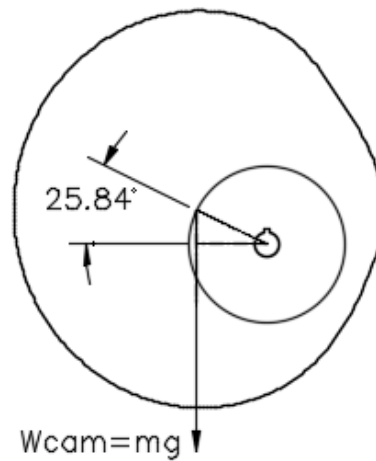*Figure 3-11 Center of gravity of the cam*

$$c = 91.8\cos(\theta + .4509)\text{mm} \qquad (101)$$

Therefore, at a lower counterweight and at the vertical position of the counterweight arm that is, θ is less, the effect of the unbalanced cam is more. But for a higher counterweight, this unbalancing effect is low.

Balancing of moments,

$$\sum M_1 = \sum M_2 \qquad (102)$$

Therefore, from (82) and (97),

$$m_{cw}L_{cw}{}^2\,\dot{\omega}+m_{cw}gL_{cw}\sin\theta = F_S R + (R^2\,\dot{\omega}+2R\frac{dR}{d\theta}\omega^2)11.53+10.37\cos(\theta+.451) \quad (103)$$

The left hand side of (103) gives the torque due to the counterweight considering its inertial affect. While the right of (103) gives the moment about the cam shaft due to payload or tension in the rope. It also considers the inertial effect and the effect of the unbalanced cam. For a higher counterweight like 400kg, as calculated in this thesis, we could neglect these effects of mass and inertia of the cam due to its low weight, i.e. 11.5 kg. For a lower counterweight, these effects are considerable and need to be calculated for accurate dynamics of the system.

3.5.   Summary of the Design of the Components

The final dimensions of the components are given below.

Table 3-3. Summary of design of components

Component	SI	Inch System
Payload	150 kg	330lbs
Counterweight	400 kg	880lbs
1. Cam		
CAM Shaft	31.25 mm	1 ¼ inch
Cam Width	63.5 mm	2 ½ inch
2. Counterweight Arm		
Square Bar	65mm x 65mm x1000 mm	2.5" x 2.5" x 39.37"
3. Gear Box		
Gear Box Shaft	27 mm	1 1/8 inch
	Gear	Pinion
Attachment	To CAM	To Payload
No of teeth	64	16

Pitch Diameter	256 mm	10 inch	64 mm	2.5 inch
Face Width	13 mm	0.5 inch	12 mm	0.5 inch
Module	4 mm		4 mm	
Diametrical Pitch		8		8

5. Spools

	Smaller Spool	Larger Spool
Diameter	2 inch	6 inch
Width	2.5 inch	3 inch (for 9.5 mm rope)

Chapter 4 - Prototype Testing

In chapter 2, we designed the cam and in chapter 3 we designed the components required for implementing the partial body-weight support system. In this chapter, we will test the prototype and will analyze the results.

For the prototype design, we tried to maintain similar sizes as designed in chapter 3. The sizes of each component used for the design are as shown in Table 4-1.

For testing, we developed and assembled the half system. That is, we manufactured and assembled one cam, one gearbox and one counterweight arm. The purpose of this was to analyze the operation of the system and to avoid any increases in the cost of testing if improvements needed to be made.

4.1. Manufacturing of Cam

The maximum diameter of the cam is 434.12 mm with a 50 mm width. Therefore, manufacturing the entire cam from a single work piece would be costly. Instead a sandwich pattern was used. Two 0.75" thick wooden cam profiles were sandwiched between three 0.25" aluminum (Al) cam profiles. These Al cam profiles were manufactured using a CNC machining center. The cam designed in section 2.3 was converted into a step file using Matlab and MSC Adams. The manufactured Al profile was used as a template for manufacturing the wooden profiles using a router. We assembled the finished sandwich of Al & wooden profiles using 0.25" bolts and nuts.

4.2. Assembly

One end of a 10-mm rope was wound on the 6" aluminum spool with the help of a ⅜"
diameter eyebolt (Refer to Figure 4-1). A wooden plate was used as a guide to the rope, so
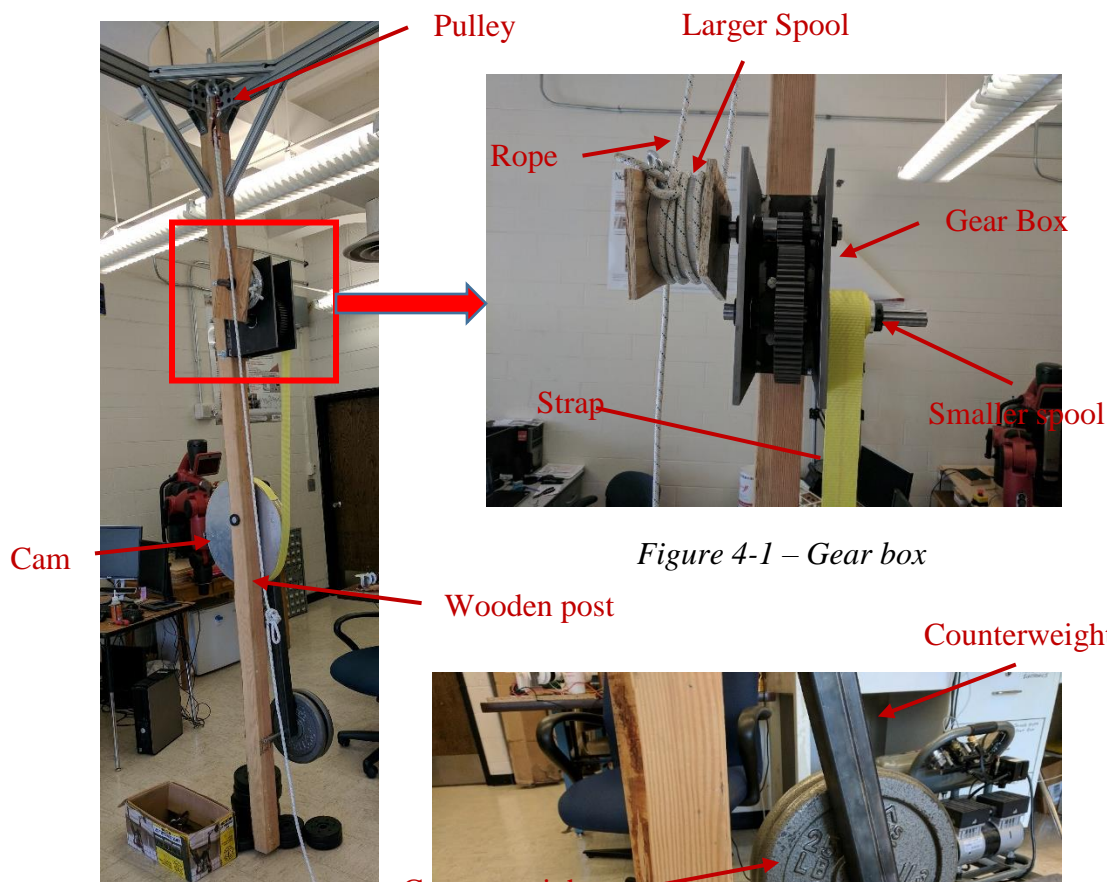that it wouldn't slip from the spool.

Figure 4-1 – Gear box
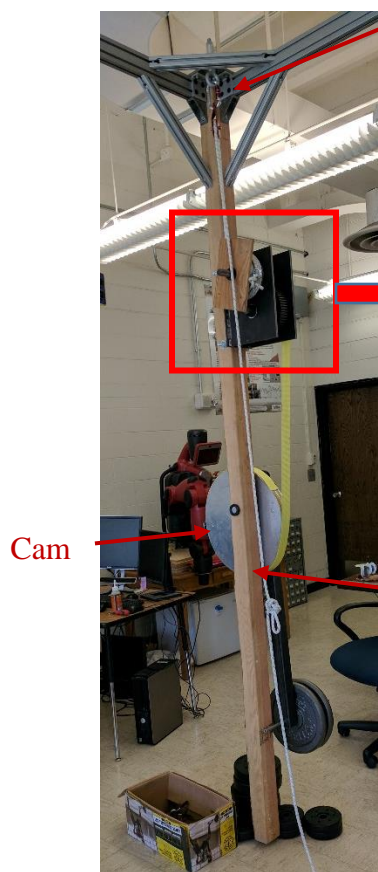
Figure 4-2 – Test setup
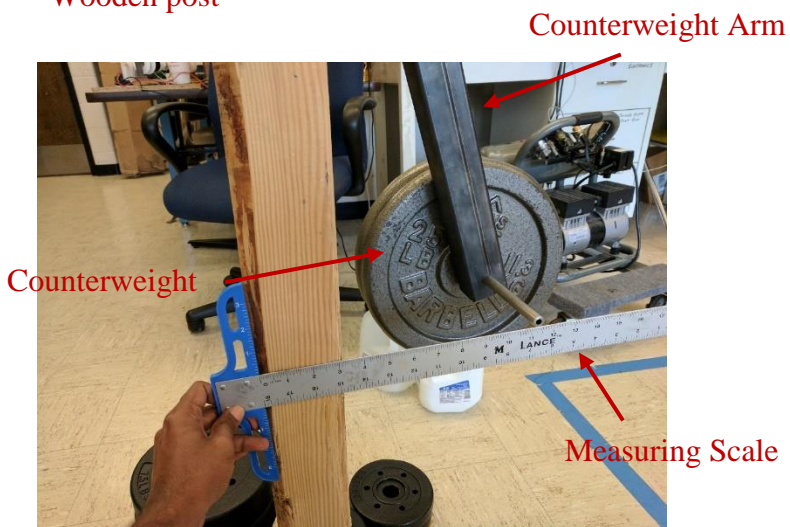
*Figure 4-3 – Counterweight and
measurement of theta by linear scale*

The other end of the rope passed through a pulley and was secured on a spring scale to measure rope tension. The pulley was assembled at a height of 120" from the ground on the main structure. The gear box, which comprised spools and gears, was assembled vertically at a height of 80" from the ground. The cam assembly, which consisted of the cam, the cam shaft, and counterweight arm, was installed on the wooden post with the help of a sleeve bearing, at a height of 50" from the ground. The nylon strap was glued on the cam and wrapped for a full revolution. It was fixed on the smaller spool with the help of three 3/16" diameter bolts 50" from the ground. See Appendix D for test setup images.

Table 4-1. Components used for testing

1. Cam

CAM Shaft	1.125"
Cam Width	2"

2. Counterweight Arm

Square tube	2" x 2" x 0.25" thick x 39.37" long

3. Gear Box

Gear Box Shaft	1"	
	Gear	Pinion
No. of teeth	64	16
Pitch Diameter	8"	2"
Face Width	2"	2"
Diametrical Pitch	8	8

4. Spools

	Smaller Spool	Larger Spool
Diameter	2 inch	6 inch
Width	2.25 inch	3 inch (for 9.5 mm rope)

4.3. Measurements

Three sets of counterweights (50 lb., 60 lb., & 70 lb.) were used to demonstrate the performance of the system. A spring scale was used to measure the tension in the rope. A protractor and tape measure were used to measure the angular position of the counterweight with respect to the wooden post. Refer to Figure 4-3.

The rope was paid out and tension in the rope was measured at specific points along the movement. The cable angle and position of payload (rope displacement) were calculated by the difference in the measuring point with respect to the starting point of the measurement.

4.4. Results

At zero counterweight, since the cam is non-circular, the center of mass of the cam tends to rotate counter-clockwise, and the system stabilizes at a counterweight angle of θ = 20°. This is a limitation of the model compared to the prototype (the model was assumed massless and the prototype was not counterbalanced to be neutral).

At a counterweight of 15 lb. (66.7 N), the counterweight arm came to a vertical position, that is, at $\theta = 0°$. The results are tabulated as shown in Table 4-2.

In Table 4-2, *y'* is the movement of the rope vertically and tension is measured at these respective points. Theta (θ) is the angle of the counterweight arm with respect to vertical. It was measured by using a tape measure and/or protractor. The readings were taken for counterweight values of 50, 60, & 70 lbs. Tension in the rope was measured using a spring scale and noted down. We observed that when the rope was fully stretched, it did

not comes back to its original position but there was some slip (related to the winding and

unwinding on the spool).

Table 4-2. Results for vertical rope movement

y'	Theta	cw	Tension
78.000	0.095	50	0.0
74.000	0.108	50	2.0
70.000	0.156	50	4.5
66.000	0.205	50	5.5
62.000	0.257	50	7.0
58.000	0.310	50	8.0
54.000	0.360	50	11.5
50.000	0.413	50	12.5
46.000	0.461	50	14.0
42.000	0.504	50	15.5
38.000	0.540	50	16.5
34.000	0.589	50	18.0
30.000	0.628	50	20.0
26.000	0.680	50	21.5
22.000	0.721	50	19.0
18.000	0.760	50	18.0
76.000	0095	60	0.0
72.000	0.115	60	2.0
68.000	0.163	60	5.0
64.000	0.216	60	6.5
60.000	0.267	60	7.5
56.000	0.321	60	10.0
52.000	0.375	60	12.0
48.000	0.425	60	13.5
44.000	0.473	60	15.0
40.000	0.518	60	14.0
36.000	0.561	60	18.5
32.000	0.603	60	20.0

y'	Theta	cw	Tension
28.000	0.647	60	20.5
24.000	0.688	60	21.5
74.000	0.095	70	0.0
70.000	0.132	70	4.0
66.000	0.182	70	6.0
62.000	0.231	70	8.0
58.000	0.283	70	10.5
54.000	0.337	70	12.0
50.000	0.391	70	13.5
46.000	0.439	70	16.0
42.000	0.486	70	17.5
38.000	0.531	70	19.0
34.000	0.574	70	20.0
30.000	0.604	70	21.0
26.000	0.660	70	22.5
22.000	0.698	70	23.5

4.5. Analysis

The data collected in *Table 4.2* do not give any conclusion regarding static and dynamic performance of the system. Therefore, to compare analytical results with experimental, we calculated torque provided by the counterweight (T_{cw}) and torque due to tension in the cable at R (T_{cable}). We calculated theoretical tension in the cable and compared it with actual tension.

4.5.1. Analysis for $y = 1.06$m, $CW = 222$N

In this section, we analyze the results for a counterweight of 50 lb (222N) and payload height of 1.06 m (y=78" from ground). The analysis steps are given below.

Table 4-3. Analysis for $h = 1.06$m, $CW = 222$N

| Sr No.	Tension	(y)	Theta	Strap Spool	R	T_{CW}	Strap Cam	T_{cable}	T_{cw}- T_{cable}	Strap Difference in mm
0	0.000	1.981	0.095	0.000	0.136	21.2	0.000	0.0	21.2	0
1	8.896	1.880	0.108	0.008	0.137	24.0	0.002	14.6	9.4	-7
2	20.017	1.778	0.156	0.017	0.138	34.6	0.008	33.2	1.4	-9
3	24.465	1.676	0.205	0.025	0.140	45.2	0.015	41.1	4.1	-10
4	31.138	1.575	0.257	0.034	0.142	56.5	0.023	53.0	3.5	-11
5	35.586	1.473	0.310	0.042	0.144	67.8	0.030	61.4	6.4	-12
6	51.155	1.372	0.360	0.051	0.146	78.4	0.038	89.4	-11.0	-13
7	55.603	1.270	0.413	0.059	0.148	89.3	0.045	98.6	-9.3	-14
8	62.275	1.168	0.461	0.068	0.150	98.9	0.052	112.0	-13.1	-15
9	68.947	1.067	0.504	0.076	0.152	107.3	0.059	125.5	-18.1	-17
10	73.396	0.965	0.540	0.085	0.153	114.4	0.065	135.0	-20.6	-20
11	80.068	0.864	0.589	0.093	0.155	123.6	0.072	149.4	-25.8	-21
12	88.964	0.762	0.628	0.102	0.157	130.6	0.078	167.9	-37.2	-23
13	95.637	0.660	0.680	0.110	0.160	139.8	0.087	183.3	-43.5	-23
14	84.516	0.559	0.721	0.119	0.162	146.9	0.093	164.1	-17.2	-25
15	80.068	0.457	0.760	0.127	0.164	153.2	0.100	157.4	-4.17	-27
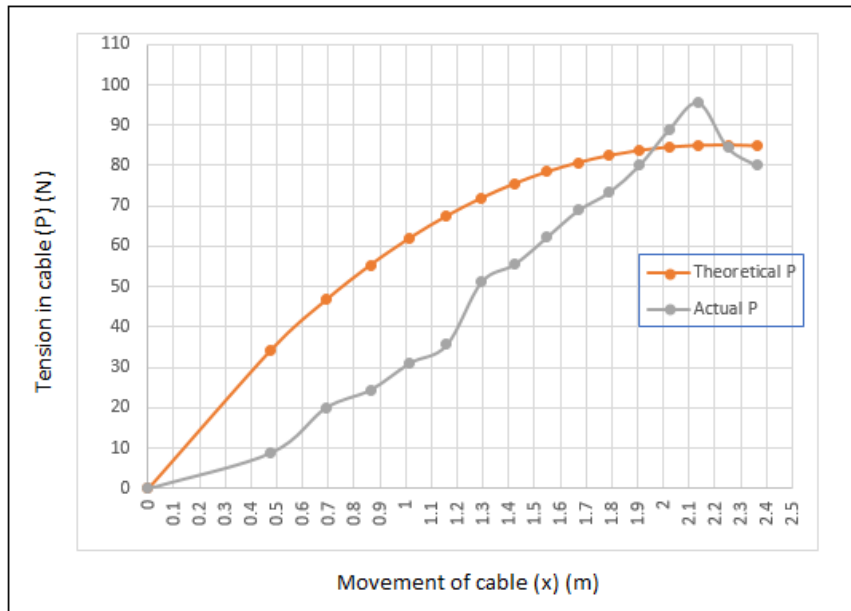
Figure 4-4 comparison between theoretical tension and actual tension in cable for Table 4-3

1. The strap displacement on the cam could be calculated from equation (14)

$$S_{CAM} = \int R(t)d\theta$$

2. The strap displacement on the smaller spool could be calculated as

$$S_{Spool} = \frac{L_{cable}}{\kappa} = \frac{L_{cable}}{12} \qquad (104)$$

3. We got an error of 27 mm at the end of the complete cycle as shown in *Table 4-3*. We got a maximum torque difference of 43.5 Nm. This difference is 31% of the torque transmitted by the cam. As seen in chapter 2, the theoretical difference between T_{cam} to T_{cable} is 1%.

4. The comparison between theoretical P and the actual tension in the cable is plotted as shown in Figure 4-4.

4.5.2. Analysis for $h = 1.12$m, $CW = 267$N

In this section, we analyze the results for a counterweight of 60 lb (267N) and payload height of 1.12 m (y=76" from ground). The analysis steps are given below.

1. The maximum difference in the strap advancement on the cam was 22 mm.

2. The maximum difference in the torque was 18 Nm which is 14% of the torque transmitted by the cam. While at the cable displacement of 2", the maximum (T_{cam}-T_{cable})/T_{cam} is 15% due to the center of gravity not passing through the axis of rotation.

3. The difference between theoretical tension and actual tension in the cable is as shown in Figure 4-5.

Table 4-4. Analysis for $h = 1.12$m, $CW = 267$N

T_{CW}	T_{cable1}	T_{cw}-T_{cable}	Strap_Spool	Strap_Cam	Strap Difference in mm	Actual Tension	Theoretical Tension
25.422	0.000	25.422	0.000	0.000	0	0.000	0.000
30.506	14.598	15.908	0.008	0.003	-6	8.896	41.228
43.217	36.943	6.274	0.017	0.009	-8	22.241	56.028
57.199	48.674	8.525	0.025	0.017	-9	28.913	66.471
70.333	56.894	13.439	0.034	0.024	-10	33.362	74.565
84.315	76.957	7.358	0.042	0.032	-10	44.482	81.070
97.873	93.707	4.166	0.051	0.040	-11	53.379	86.368
110.160	106.890	3.270	0.059	0.047	-12	60.051	90.683
121.600	120.370	1.229	0.068	0.054	-13	66.723	94.162
132.192	113.803	18.389	0.076	0.061	-15	62.275	96.912
141.937	152.243	-10.306	0.085	0.068	-17	82.292	99.011
151.258	166.612	-15.354	0.093	0.074	-19	88.964	100.526
160.825	173.036	-12.211	0.102	0.081	-20	91.189	101.516
169.477	183.766	-14.289	0.110	0.088	-22	95.637	102.035

Figure 4-5 Comparison between theoretical tension and actual tension in cable for
Table 4-4
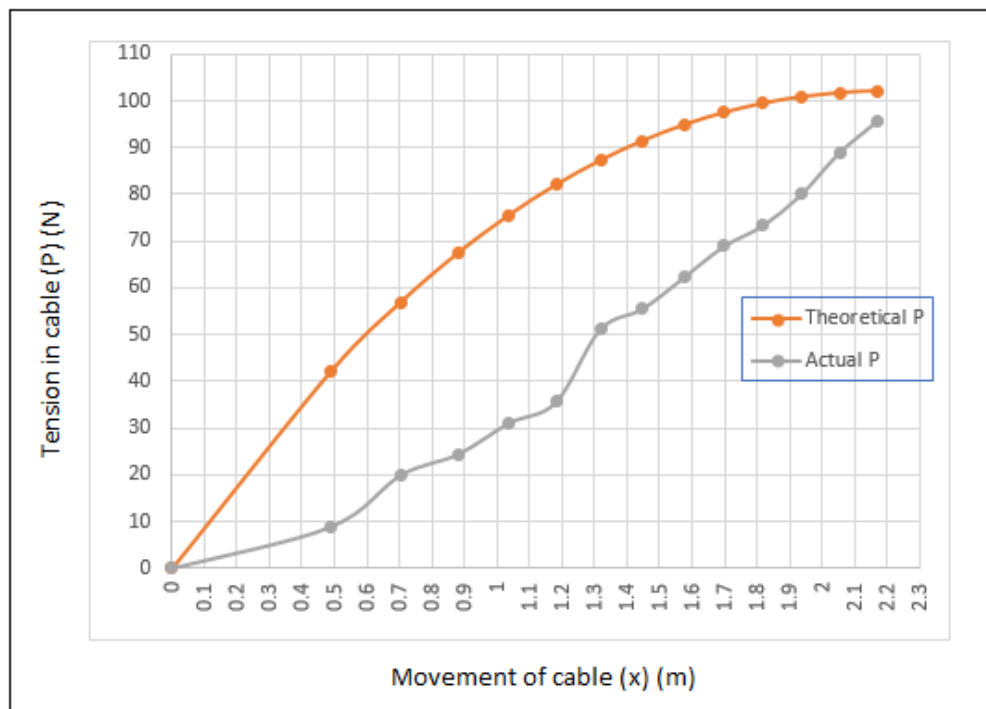
4.5.3.   Analysis for $h = 1.17$m, $CW = 311$N

In this section, we analyze the results for a counterweight of 60 lb (267N) and payload height of 1.12 m (y=76" from ground). The analysis steps are given below.

1. The maximum difference in the strap advancement on the cam was 21 mm.

2. The maximum difference in the torque was 12 Nm. This is 10% of the torque transmitted by the cam. For the cable displacement of 4", this difference is 12% due to improper center of mass of the cam.

3. The difference between the theoretical tension and the actual tension in the cable is as shown in Figure 4-6.

Table 4-5. Analysis at $h = 1.17$m, $CW = 311$N

| T_{CW}	T_{cable1}	T_{cw}-T_{cable}	Strap_Spool	Strap_Cam	Strap Difference in mm	Actual Tension	Theoretical Tension
29.658	0.000	29.658	0.000	0.000	0	0.000	0.000
41.027	29.196	11.699	0.008	0.005	-3	17.793	49.934
56.350	44.331	11.803	0.017	0.012	-5	26.689	67.548
71.179	59.906	11.050	0.025	0.019	-7	35.586	79.823
86.997	79.652	7.003	0.034	0.026	-8	46.706	89.227
102.814	92.348	10.092	0.042	0.034	-8	53.379	96.694
118.632	105.421	12.764	0.051	0.042	-9	60.051	102.696
132.472	126.685	5.290	0.059	0.049	-10	71.172	107.512
145.324	140.432	4.391	0.068	0.056	-12	77.844	111.327
157.682	154.447	2.663	0.076	0.063	-13	84.516	114.272
169.050	164.587	3.830	0.085	0.070	-15	88.964	116.448
176.959	174.943	1.917	0.093	0.075	-19	93.413	117.940
190.800	189.917	0.147	0.102	0.083	-18	100.085	118.823
200.191	200.861	-1.310	0.110	0.090	-21	104.533	119.166
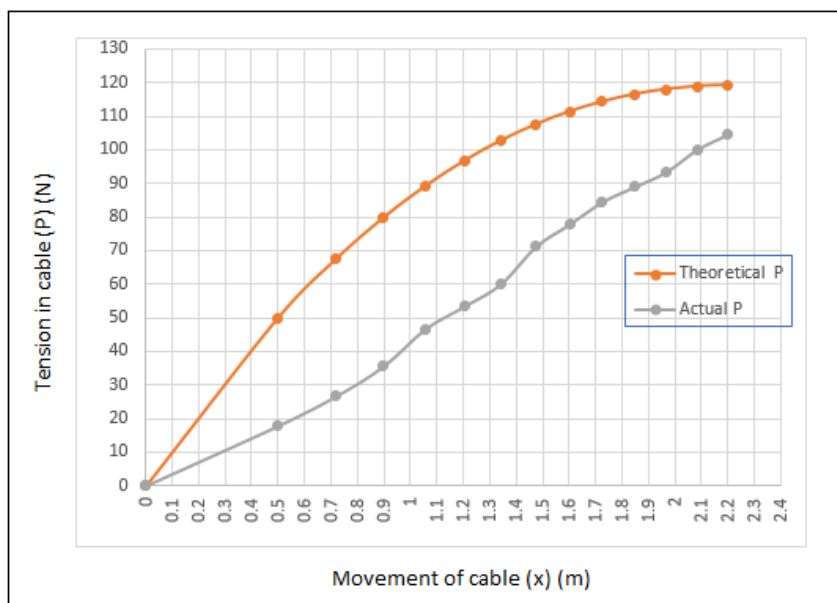
Figure 4-6 Comparison between theoretical tension and actual tension in cable for Table 4-5

4.6. Observations and Conclusions

1. The center of mass of the cam does not pass through the axis of rotation of the cam. Therefore, the tension in the rope will always be less than the theoretical calculated tension in the rope. This explained some of the error in the previous figures.

2. For larger movement of the cable, the difference between the actual tension and the calculated tension was relatively low, in the range of 12%. Table 4-6 shows the difference in percentage of tensions for each case.

3. In Table 4-6, y'' is the position of the spring scale for reference. That is, $y''_1 - y''_2$ is the cable displacement. We took measurements at intervals of 4" cable displacement. Columns labeled 50 lb., 60 lb., and 70 lb. show the ratio given by

$$\frac{P_{Actual} - P_{Theroetical}}{P_{Theroetical}} \% \qquad (105)$$

Table 4-6. Percentage difference in tensions in cable

y"	50 lb	60 lb	70lb
74	74%		
70	57%	79%	
66	56%	61%	63%
62	50%	57%	59%
58	47%	56%	54%
54	29%	46%	46%
50	26%	39%	44%
46	21%	34%	40%
42	15%	30%	33%
38	11%	36%	29%
34	4%	17%	25%
30	-5%	12%	23%
26	-12%	10%	20%
22	1%	6%	15%
18	6%		12%

4. The installation of the strap and rope should be done under proper tension.

   Furthermore, we could not adjust tension easily, since there was no brake attached to

   the gearbox. Therefore, one of the design improvements will be the locking of the

   gear box so that the rope and strap can be installed easily.

Chapter 5 - Conclusions and Future Work

This thesis presents the design and testing of a "Cam-Based Pose-Independent Counterweighting for Partial Body-Weight Support in Rehabilitation" in a two-dimensional work space.

We have discussed that the gait dysfunctions are changes in normal walking patterns, often related to a disease or abnormality in different areas of the body. There are numerous body-weight support (BWS) systems like "The Treadmill Body-Weight Support System" or the "Multidirectional Transparent Support System" which are applied to rehabilitation during gait training. But most of these BWS systems are costly and generally are stationary devices. A major drawback of such devices is the lack of degrees of freedom for free ambulation. While some multidirectional body-weight support systems do exist, these devices are equipped with sensors and control systems which increase the cost of the product.

The main objective of this project was to introduce a partial body-weight support system which can be used in a three-dimensional work space. But the scope of this thesis is limited to verify the concept in a two-dimensional work space and test and verify the prototype. Also, another objective of the research is development of a low-cost weight-offload system which is easy to operate, flexible in its installation footprint, and requires little to no electromechanical input.

We proposed a cable-based body-weight support system which allows the user to move in a two-dimensional workspace with a uniform supporting force throughout that workspace. This was achieved by coupling the cable displacements to the counterweight

displacements using mechanical programming via cams. There would be two identical sets of cams, gear boxes and counterweights to support the uniform force on the payload.

The design of the cam was a complex process due to the involvement of implicit equations which could not be solved explicitly. This work was restricted by the assumptions that a patient walks in a straight line and there are no forces or movement in another direction. Using a planar system of two cables suspended from two anchoring positions, the system was balanced. Cable tensions were related to payload and displacement. The length of the cable to be wrapped on the pulley was related to the radius of the cam and the displacement of the payload. Since these variables are interdependent and implicit, a trial and error method was used. We had assumed the initial value of $R(\theta)$ and solved these equations. Then we changed the assumed value so that all the equations were satisfied. For this we used Excel for solving by the trial and error method. The cam profile was achieved by fitting a six-degree polynomial to the resulting $R(\theta)$. This cam was designed for a reference height of 1.05 m from the top of the support frame for a maximum payload of 150 kg and counterweight of 400 kg.

With this approach, as designed and built, torque was not fully balanced. We also got a difference of 1% torque at the designed parameters. This difference increased to 15% for payload positions moved 0.3 m either upwards or downwards for change in the counterweight value. If we keep the same counterweight as 400 kg, these differences increase to 35%. Therefore, there is need of compensatory torque to balance the system.

To verify this design, a prototype was built in the lab and tested. It is observed that:

- The center of mass location of the cam affects the tension in the rope to around 70% of the designed torque for lower counterweight, and it decreases as we increase the counterweight. Since the system was tested to a maximum 70 lb. of counterweight instead of the designed 880 lb., this effect may be negligible in practice.

- Since testing was done on a relative lower counterweight, the system mass affects the recorded calculation.

- The actual tension follows an incremental path as designed, and the profile is similar to the theoretical tension; therefore it appears that the calculation of the cam profile holds true.

- As we observed that torque differences in the cable and cam shaft decrease with an increase in counterweight, we can accept the calculations and design, pending further testing.

Future Work:

The following modifications need to be done before moving into a three-dimensional workspace:

- Balancing of the cam. It has a significant effect on torque and tension in the cable at lower counterweights. The balancing of the cam can be done by the addition of mass.

- A mechanism to measure tension at a higher counterweight. We need to take more readings at much higher counterweights to validate the system. A winch for holding the rope at high counterweight values and appropriate load cells in-line with the rope can be used to measure accurate tension in the rope.

- Improved methodology is needed to measure the angle of the cam with greater precision. Digital angular sensors like potentiometers can be used for this purpose.

- Development of a full two-dimensional system and observation of changes in tension in both the cables. Since, in the current phase, testing of the prototype was done in a half-system model, it would be beneficial to see the behavior of a complete two-dimensional system before arriving at particular conclusions to pursue the 3-dimensional workspace.

- Mechanism to assemble a gear box with brake. This will help for assembling the system. Also, it is useful for attaching and detaching payload from the system in case of an emergency.

References

[1] K. H. Low, "Recent Development and Trends of Clinical-Based Gait Rehabilitation Robots," in *Intelligent Assistive Robots: Recent Advances in Assistive Robotics*, Cham, Springer, 2015.

[2] J. H. Matsubara, M. Wu and K. E. Gordon, "Metabolic cost of lateral stabilization during walking in people with incomplete spinal cord injury," *Gait & posture,* vol. 41, pp. 646-651, Feb 2015.

[3] S. Mohammed, J. C. Moreno, K. Kong, Y. Amirat and editors, Intelligent assistive robots : recent advances in assistive robotics for everyday activities, Cham, : Springer, 2015.

[4] S. B. OŚullivan, Physical rehabilitation, 5th ed., F- Davis, 2007, pp. 61-68.

[5] E. J. Protas, K. Mitchell, A. Williams, H. Qureshy, K. Caroline and E. C. Lai, "Gait and step training to reduce falls in Parkinsoń disease," *NeuroRehabilitation,* vol. 20, pp. 183-190, 2005.

[6] B. Salzman, "Gait and balance disorders in older adults," *Am Fam Physician,* vol. 82, p. 61, July 2010.

[7] K. Kubo, T. Miyoshi, A. Kanai and K. Terashima, "Gait Rehabilitation Device in Central Nervous System Disease: A Review," *Journal of Robotics,* vol. 2011, pp. 1-14, 2011.

[8] J. E. Deutsch, R. F. Boian and G. C. Burdea, "Chapter-3: Robotics and Virtual Reality Applications in Mobility Rehabilitation," in *Rehabilitation Robotics*, S. S. Kommu, Ed., I-Tech Education and Publishing, 2007.

[9] K. J. Dodd and S. Foley, "Partial body-weight-supported treadmill training can improve walking in children with cerebral palsy: a clinical controlled trial," *Developmental medicine and child neurology,* vol. 49, pp. 101-105, Feb 2007.

[10] J. Hidler, W. Wisman and N. Neckel, "Kinematic trajectories while walking within the Lokomat robotic gait-orthosis," *Clinical Biomechanics,* vol. 23, pp. 1251-1259, 2008.

[11] C. Nelson, R. Thienpont and A. Shinde, "Pose-independent counterweighting of cable-suspended payloads with application to rehabilitation.," *New Trends in Mechanism and Machine Science Mechanisms and Machine Science,* July 2016.

[12] C. A. Nelson, J. M. Burnfield, Y. Shu, T. W. Buster, A. P. Taylor and A. Graham, "Modified Elliptical Machine Motor-Drive Design for Assistive Gait Rehabilitation," *Journal of Medical Devices,* vol. 5, p. 21001, 2011.

[13] J. M. Burnfield, S. L. Irons, T. W. Buster, A. P. Taylor, G. A. Hildner and Y. Shu, "Comparative analysis of speeds impact on muscle demands during partial body weight support motor-assisted elliptical training," *Gait \& posture,* vol. 39, pp. 314-320, 2014.

[14] J. M. Burnfield, Y. Shu, T. W. Buster, A. P. Taylor and C. A. Nelson, "Impact of Elliptical Trainer Ergonomic Modifications on Perceptions of Safety, Comfort, Workout, and Usability for People With Physical Disabilities and Chronic Conditions," *Physical Therapy,* vol. 91, pp. 1604-1617, Nov 1, 2011.

[15] J. M. Burnfield, Y. Shu, T. Buster and A. Taylor, "Similarity of Joint Kinematics and Muscle Demands Between Elliptical Training and Walking: Implications for Practice," *Physical Therapy,* vol. 90, pp. 289-305, Feb 1, 2010.

[16] M. Frey, G. Colombo, M. Vaglio, R. Bucher, M. Jorg and R. Riener, "A Novel Mechatronic Body Weight Support System," *IEEE Transactions on Neural Systems and Rehabilitation Engineering,* vol. 14, pp. 311-321, 2006.

[17] A. C. Dragunas and K. E. Gordon, "Body weight support impacts lateral stability during treadmill walking," *Journal of Biomechanics,* vol. 49, pp. 2662-2668, Sep 2016.

[18] V. Rajasekaran, J. Aranda, A. Casals and J. L. Pons, "An adaptive control strategy for postural stability using a wearable robot," *Robotics and Autonomous Systems,* vol. 73, pp. 16-23, Nov 2015.

[19] D. J. Reinkensmeyer and V. Dietz, Neurorehabilitation Technology, Second edition. ed., Cham, : Springer Verlag, 2016.

[20] M. K. Aaslund and R. Moe-Nilssen, *Treadmill walking with body weight support,* vol. 28, 2008, pp. 303-308.

[21] D. Sharan, J. S. Rajkumar, R. Balakrishnan, A. Kulkarni, K. Selvakumar, S. Gampa, M. Mohandoss and R. Ranganathan, "Effectiveness of a low-cost body weight support training device in the rehabilitation of cerebral palsy," *Journal of*

Rehabilitation and Assistive Technologies Engineering, vol. 3, p. 205566831667604, Nov 2016.

[22] H. Vallery, P. Lutz, J. von Zitzewitz, G. Rauter, M. Fritschi, C. Everarts, R. Ronsse, A. Curt and M. Bolliger, "Multidirectional transparent support for overground gait training," *IEEE ... International Conference on Rehabilitation Robotics : [proceedings],* vol. 2013, p. 6650512, Jun 2013.

[23] A. B. Alp and S. K. Agrawal, "Cable suspended robots: design, planning and control," 2002.

[24] V. Arakelian, "Gravity compensation in robotics," *Advanced Robotics,* vol. 30, pp. 79-96, Jan 17, 2016.

[25] J. L. Herder, "Energy-free systems: theory, conception, and design of statically balanced spring mechanisms," 2001.

[26] J. Wang and C. M. Gosselin, "Static balancing of spatial three-degree-of-freedom parallel mechanisms," *Mechanism and Machine Theory,* vol. 34, pp. 437-452, 1999.

[27] S. C. Chapra and R. P. Canale, Numerical methods for engineers, 6th ed. ed., Boston, : McGraw-Hill Higher Education, 2010.

[28] R. G. Budynas, J. K. Nisbett and J. E. Shigley, Shigleyś mechanical engineering design, 9th ed., New, York: McGraw-Hill, 2011.

[29] E. J. Hearn, Mechanics of Materials Volume 1 : An Introduction to the Mechanics of Elastic and Plastic Deformation of Solids and Structural Materials, vol. 3rd ed, Oxford, : Butterworth-Heinemann, 1997.

[30] W. C. Young, R. G. Budynas, A. M. Sadegh and R. J. Roark, Roarkś formulas for stress and strain, 8th ed., New York : McGraw-Hill, 2012.

[31] F. Pfeiffer and T. Schindler, Introduction to dynamics, Berlin: Springer, 2015.

[32] O. M. OŔeilly, Engineering dynamics, 2nd ed., New, York: Springer, 2010.

[33] R. L. Waters and S. Mulroy, "The energy expenditure of normal and pathologic gait," *Gait & posture,* vol. 9, pp. 207-231, July 01 1999.

Appendix

Appendix A – Cam Design

A - 1: Matlab Code to Find Complete CAM profile

```
clc;
clear all;
close all;


theta = [0:(pi./360):(2.*pi)];



A =  find(theta <= ((5.*pi)/12));
   R1 = -(0.0708.*(theta(1,A).^6))+(0.2856.*(theta(1,A).^5))-
(0.404.*(theta(1,A).^4))+(0.2702.*(theta(1,A).^3))-(0.078.*(theta(1,A).^2))+(0.0447.*theta(1,A))+0.1323;

B = find(((5.*pi)/12) < theta );
   R2 = (0.0098705631176298.*(theta(1,B).^3))-
(0.124487286387676.*(theta(1,B).^2))+(0.440030738865897*theta(1,B))-0.166328882873349;

 Z = 5.*zeros( length(theta),1);

Cam_R = [R1 R2]

plot3( Cam_R.*cos(theta), Cam_R.*sin(theta),Z);

CAM = [theta, Cam_R.*cos(theta), Cam_R.*sin(theta),Z];

save CAM.dat CAM  -ascii

polar(theta, Cam_R)
```
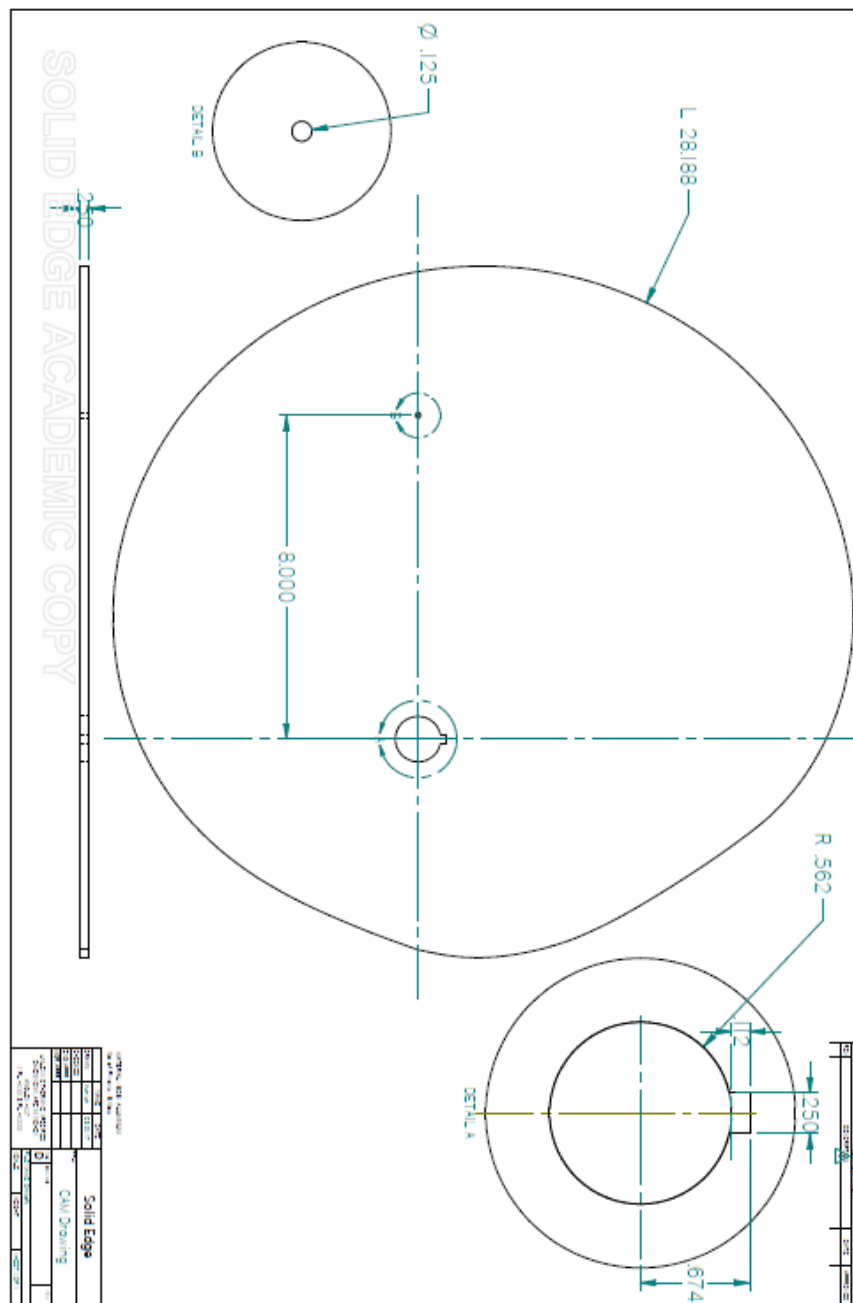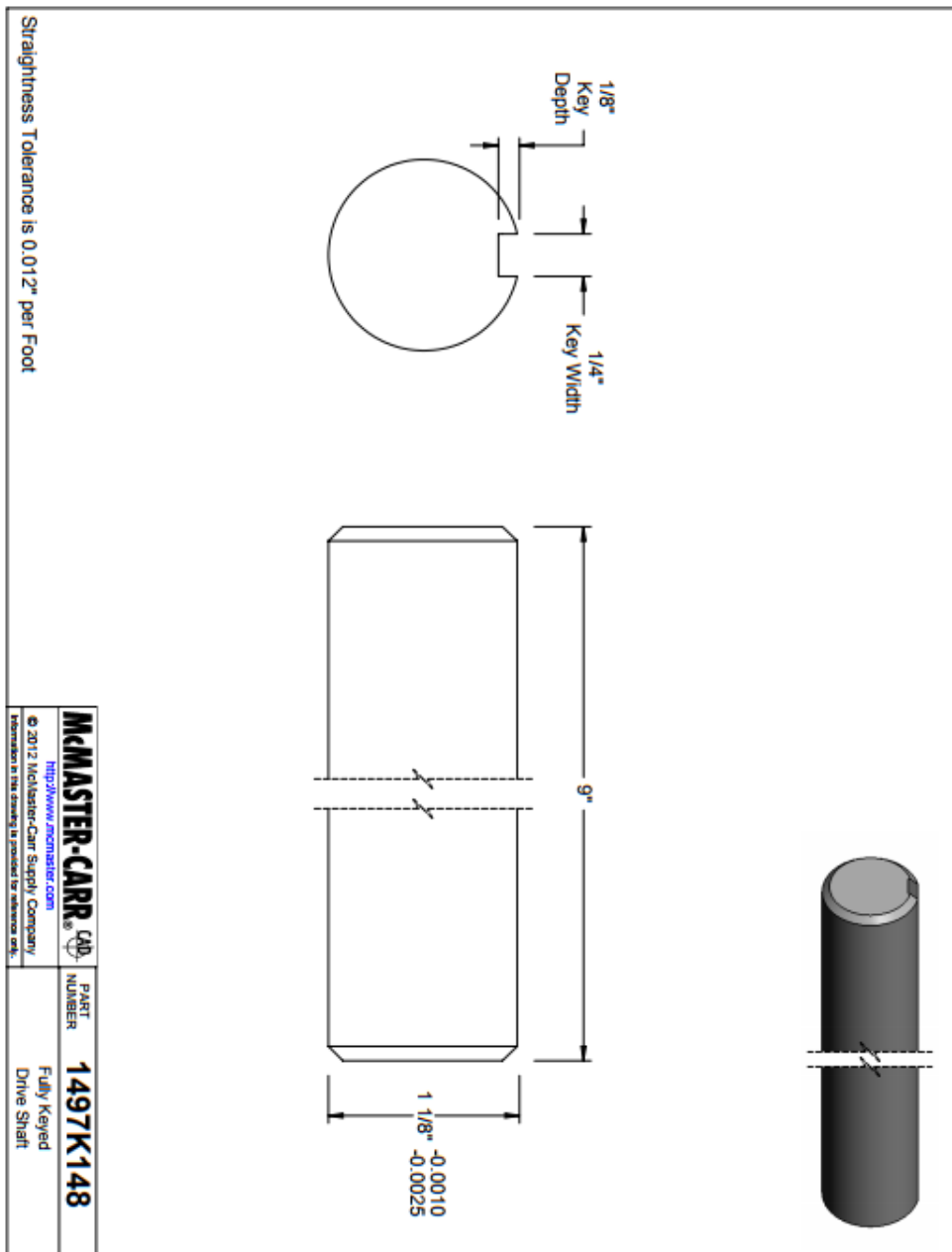
A - 2:   CAM Profile (2D Drawing)

A - 3: CAM Shaft

Straightness Tolerance is 0.012" per Foot

1/8"
Key
Depth

1/4"
Key Width

9"

1 1/8"   -0.0010
         -0.0025

PART NUMBER 1497K148

Fully Keyed
Drive Shaft

A - 4: Sleeve Bearing

1.125"±0.001

1 3/8" +0.003 +0.002

4"±0.005

For 1 1/8" Shaft Dia.

McMASTER-CARR CAD

http://www.mcmaster.com

© 2015 McMaster-Carr Supply Company

Information in this drawing is provided for reference only.

PART NUMBER 6381K251

Multipurpose Sleeve Bearing
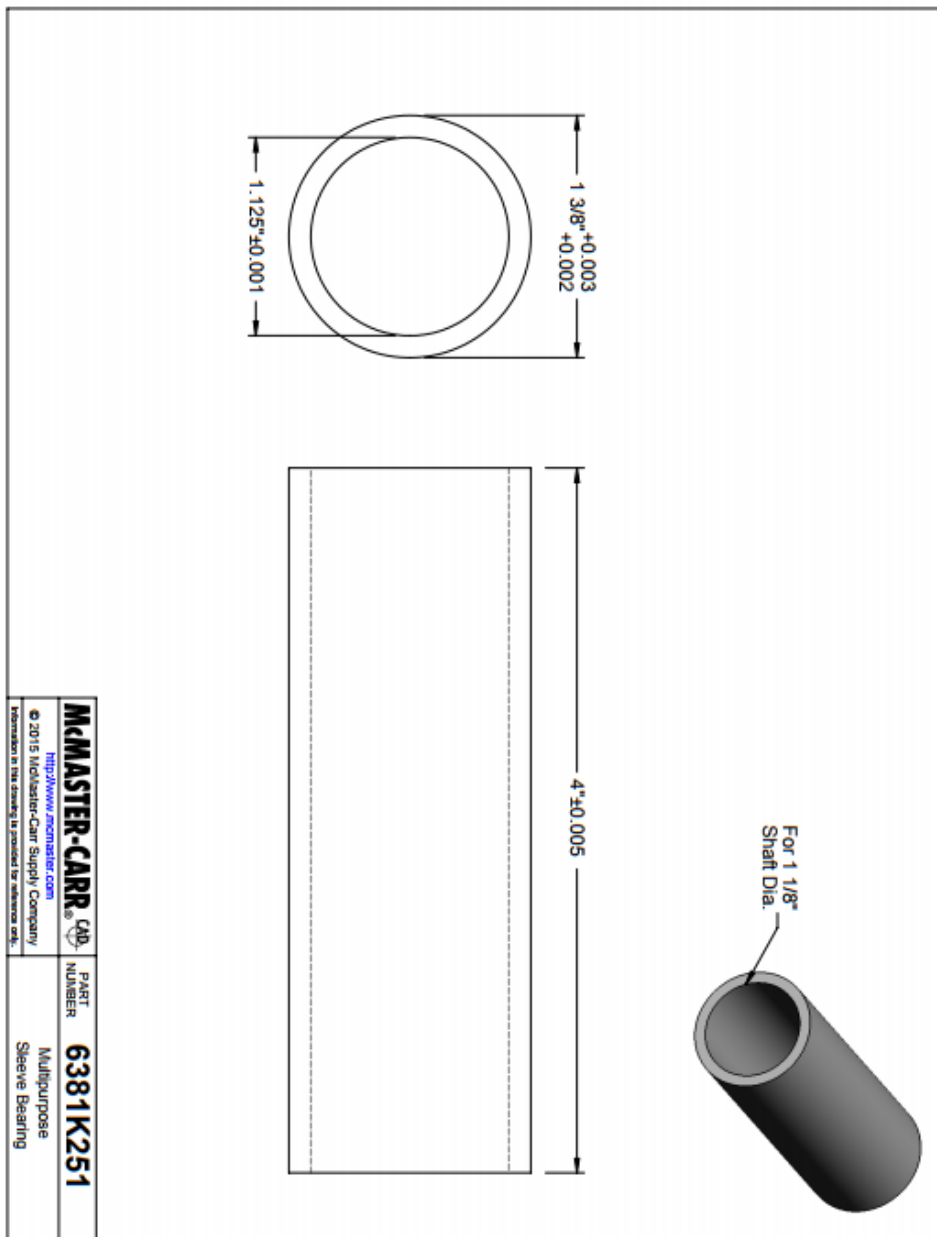
A - 5: CAM – MED Data

1.   Cam – Al profile

Physical Properties   ✕

☐ User-defined properties

Global Principal

Coordinate system:
Base   ⌄

Mass:
2.665 kg

Volume:
982680.992 mm^3

Surface area:
319080.16 mm^2

Material

Name:
Aluminum, 1060

Density:
2712.000 kg/m^3

Change

Center of Mass   cm
☐ Display symbol ●

X: -82.63 mm
Y: 40.01 mm
Z: 0.00 mm

Center of Volume   cv
☐ Display symbol ●

X: -82.63 mm
Y: 40.01 mm
Z: 0.00 mm

Accuracy (0 to 1.0):
0.99 ⬍

☑ Update on file save

Mass Moments of Inertia

Ixx:
0.040 kg-m^2

Iyy:
0.049 kg-m^2

Izz:
0.089 kg-m^2

Ixy:
-0.009 kg-m^2

Ixz:
0.000 kg-m^2

Iyz:
0.000 kg-m^2

Update   Close   Save As...   Help

2.   Cam – Wooden profile

Appendix B – Gear Box Design

B - 1:   Spur Gears from Boston

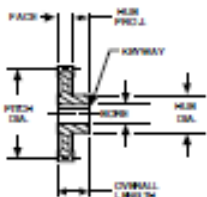Source**:** http://www.bostongear.com/

Spur Gears

10 and 8 Diametral Pitch (Cast Iron, Steel & Non-Metallic)
14-1/2° Pressure Angle (will not operate with 20° spurs)

A

STANDARD TOLERANCES

DIMENSION		TOLERANCE
BORE	All	+.0005

10 D.P.   8 D.P.

REFERENCE PAGES

Alterations — 322
Horsepower Ratings — 54, 55
Lubrication — 322
Materials — 323
Selection Procedure — 49

*Special Pitch Diameter, used for calculating Center Distance only, not Ratio.

†All gears have standard keyway, at 90° to setscrew. See Page 325.

ALL DIMENSIONS IN INCHES
ORDER BY CATALOG NUMBER OR ITEM CODE

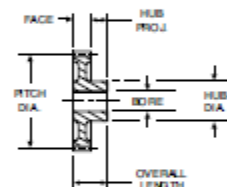| No. of Teeth	Pitch Dia.	Bore	Hub Dia.	Hub Proj.	Style Size Page 325	Without Keyway or Setscrew Catalog Number	Without Keyway or Setscrew Item Code	With Keyway and Setscrew† Catalog Number	With Keyway and Setscrew† Item Code
10 DIAMETRAL PITCH						Face = 1.000" Outside Dia. = Pitch Dia. + .200" Overall Length = 1.000" + Hub Proj.			
CAST IRON									
40	4.000					NF40	10320	–	–
42	4.200					NF42	10322	–	–
45	4.500				B	NF45	10324	–	–
48	4.800					NF48	10326	–	–
50	5.000					NF50	10328	–	–
54	5.400	.875	2.12	.88	C	NF54	10330	–	–
55	5.500					NF55	10332	–	–
60	6.000					NF60	10334	–	–
64	6.400					NF64	10336	–	–
70	7.000					NF70	10338	–	–
72	7.200					NF72	10340	–	–
80	8.000					NF80	10342	–	–
84	8.400					NF84	10344	–	–
90	9.000		2.25		D	NF90	10346	–	–
96	9.600					NF96	10348	–	–
100	10.000		2.25	.88		NF100	10350	–	–
110	11.000					NF110	10352	–	–
120	12.000					NF120	10356	–	–
140	14.000	1.00	2.50	1.00		NF140	10358	–	–
144	14.400					NF144	10360	–	–
160	16.000					NF160	10362	–	–
180	18.000		2.75			NF180	10364	–	–
8 DIAMETRAL PITCH						Face = 1.250" Outside Dia. = Pitch Dia. + .250" Overall Length = 1.250" + Hub Proj.			
STEEL									
11	1.500*		1.12			NH11B	09806	NH11B-3/4	46093
12	1.500	.750	1.12	.75		NH12B	09808	NH12B-3/4	46094
14	1.750		1.31			NH14B	09810	NH14B-3/4	46095
15	1.875	.875	1.43	.75		NH15B	09812	NH15B-7/8	46096
16	2.000	.875 / 1.000	1.56	.75		NH16B	09814	NH16B-7/8	46097
						–	–	NH16B-1	46098
18	2.250	.875 / 1.000 / 1.125	1.81	.75		NH18B	09816	NH18B-7/8	46099
						–	–	NH18B-1	46100
						–	–	NH18B-1-1/8	46101
20	2.500	.875 / 1.000 / 1.125	2.06	.75	A	NH20B	09818	NH20B-7/8	46102
						–	–	NH20B-1	46103
						–	–	NH20B-1-1/8	46104
22	2.750	.875 / 1.000 / 1.125	2.31	.75		NH22B	09820	NH22B-7/8	46105
						–	–	NH22B-1	46106
						–	–	NH22B-1-1/8	46107
24	3.000		2.06			NH24A	10368	–	–
28	3.500	.875	2.56	.88		NH28A	10370	–	–
30	3.750		2.75			NH30A	10372	–	–
32	4.000	1.000	3.00	.88		NH32A	10374	–	–
NON-METALLIC									
16	2.000	.750	1.62	.75		QHH16	09082	–	–
18	2.250		1.88			QHH18	09084	–	–
20	2.500		2.12		A	QHH20	09086	–	–
24	3.000	.875	2.62	.75		QHH24	09088	–	–
28	3.500		3.12			QHH28	09090	–	–

Spur Gears

8 and 6 Diametral Pitch (Cast Iron & Steel)
14-1/2° Pressure Angle (will not operate with 20° spurs)

A

ALL DIMENSIONS IN INCHES
ORDER BY CATALOG NUMBER OR ITEM CODE

No. of Teeth	Pitch Dia.	Bore	Hub Dia.	Hub Proj.	Style See Page 323	Without Keyway or Setscrew Catalog Number	Without Keyway or Setscrew Item Code	With Keyway and Setscrew† Catalog Number	With Keyway and Setscrew† Item Code
8 DIAMETRAL PITCH						Face = 1.250"			
						Outside Dia. = Pitch Dia. + .250"			
						Overall Length = 1.250" + Hub Proj.			
CAST IRON									
36	4.500					NH36	10376	–	–
40	5.000					NH40	10378	–	–
42	5.250				B	NH42	10380	–	–
44	5.500					NH44	10382	–	–
48	6.000					NH48	10384	–	–
54	6.750	1.000	2.50	1.00	C	NH54	10386	–	–
56	7.000					NH56	10388	–	–
60	7.500					NH60	10390	–	–
64	8.000					NH64	10392	–	–
72	9.000					NH72	10394	–	–
80	10.000					NH80	10396	–	–
84	10.500					NH84	10398	–	–
88	11.000				D	NH88	10400	–	–
96	12.000					NH96	10402	–	–
112	14.000	1.125	3.00	1.12		NH112	10404	–	–
120	15.000					NH120	10406	–	–
128	16.000					NH128	10408	–	–
144	18.000					NH144	10410	–	–
160	20.000	1.125	3.25	1.25		NH160B	10412	–	–
6 DIAMETRAL PITCH						Face = 1.500"			
						Outside Dia. = Pitch Dia + .333"			
						Overall Length = 1.500" + Hub Proj.			
STEEL									
11	2.000*	1.000	1.46	.88		NJ11B	09830	NJ11B-1	46108
12	2.000					NJ12B	09832	NJ12B-1	46109
14	2.333	1.000	1.79	.88		NJ14B	09834	NJ14B-1	46110
		1.125				–	–	NJ14B-1-1/8	46111
15	2.500	1.000	1.96	.88		NJ15B	09836	NJ15B-1	46112
		1.125				–	–	NJ15B-1-1/8	46113
		1.1875				–	–	NJ15B-1-3/16	46114
		1.250				–	–	NJ15B-1-1/4	46115
16	2.667	1.000	2.13	.88		NJ16B	09838	NJ16B-1	46116
		1.125			A	–	–	NJ16B-1-1/8	46117
		1.1875				–	–	NJ16B-1-3/16	46118
		1.250				–	–	NJ16B-1-1/4	46119
18	3.000	1.000	2.46	.88		NJ18B	09840	NJ18B-1	46120
		1.125				–	–	NJ18B-1-1/8	46121
		1.1875				–	–	NJ18B-1-3/16	46122
		1.250				–	–	NJ18B-1-1/4	46123
20	3.333	1.000	2.79	.88		NJ20	09842	NJ20-1	46124
		1.125				–	–	NJ20-1-1/8	46125
		1.1875				–	–	NJ20-1-3/16	46126
		1.250				–	–	NJ20-1-1/4	46127
21	3.500	1.000	2.96	.88		NJ21B	09844	–	–
24	4.000		3.00			NJ24A	10414	–	–
27	4.500	1.125	3.50	.88		NJ27A	10416	–	–
30	5.000		4.00			NJ30A	10418	–	–

STANDARD TOLERANCES

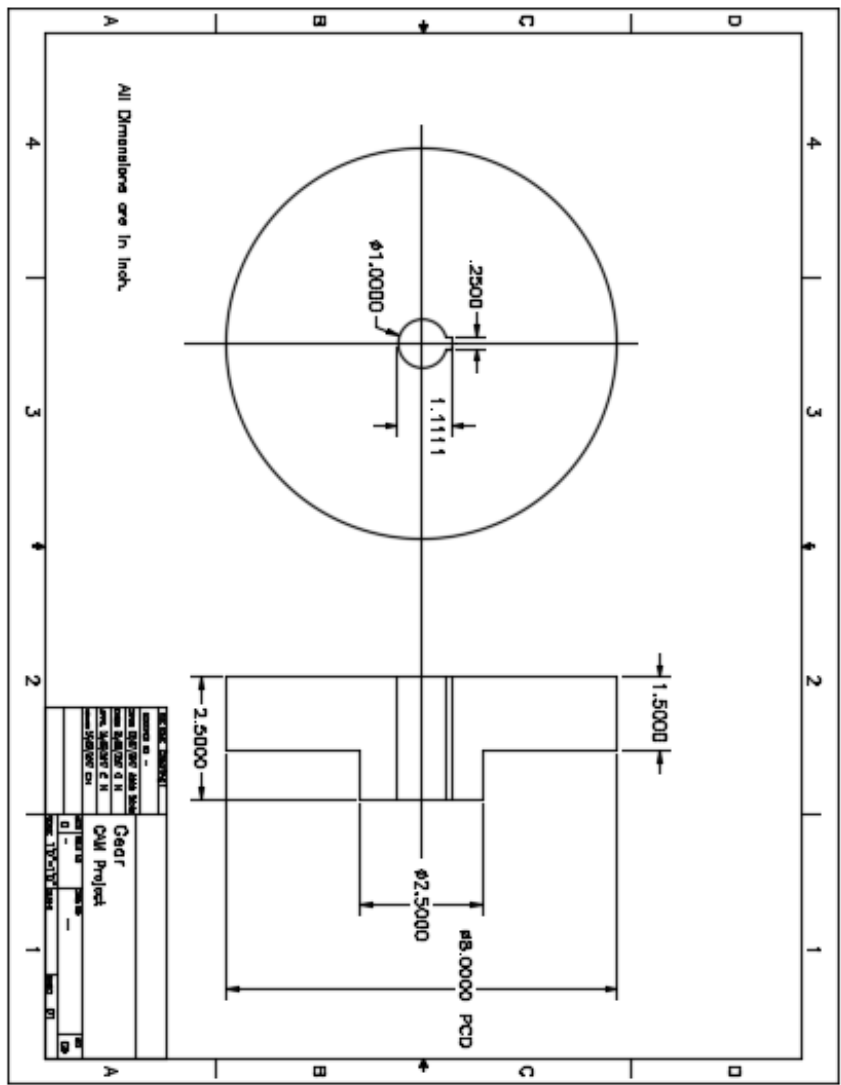| DIMENSION		TOLERANCE
BORE	All	±.0005

8 D.P.   6 D.P.

REFERENCE PAGES

Alterations — 322
Horsepower Ratings — 55, 56
Lubrication — 322
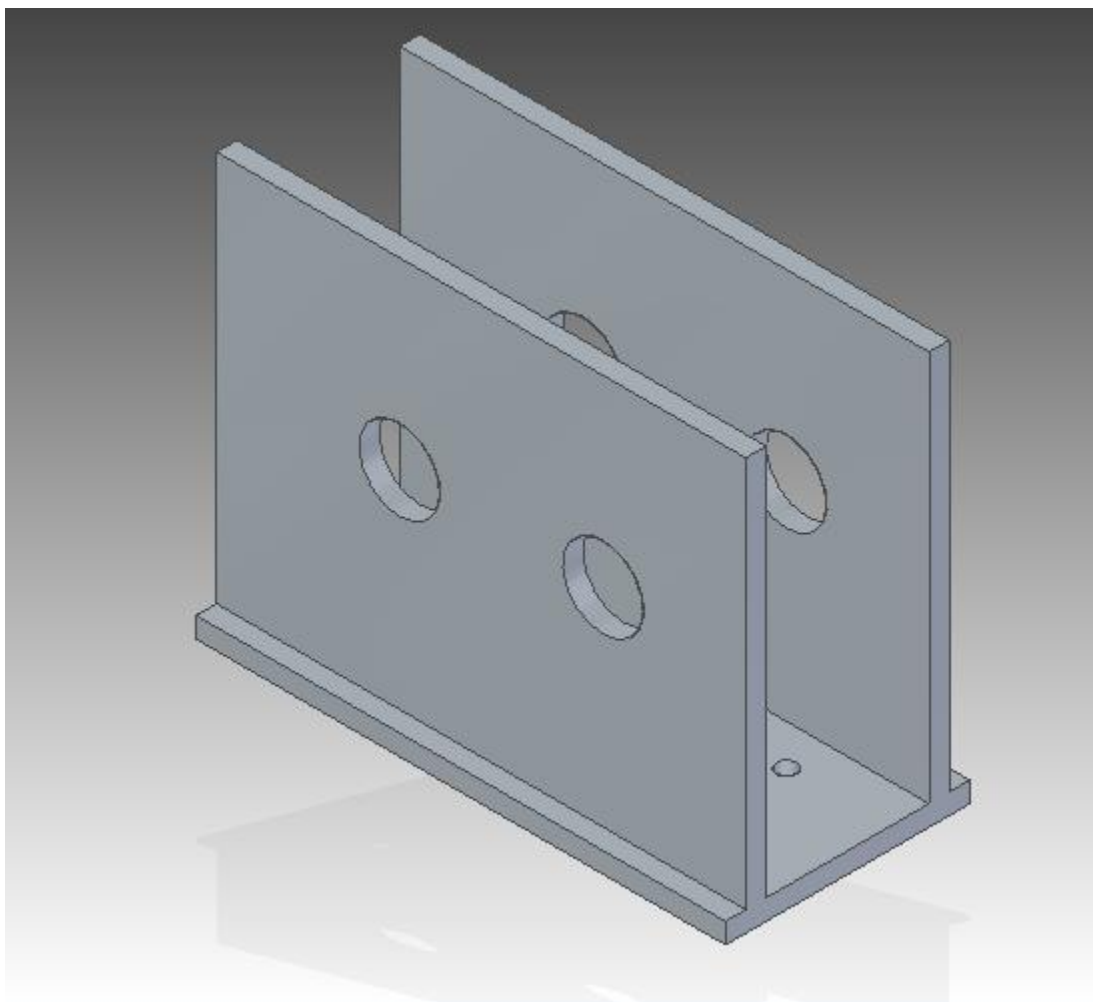Materials — 323
Selection Procedure — 49

*Special Pitch Diameter, used for calculating Center Distance only, not Ratio.

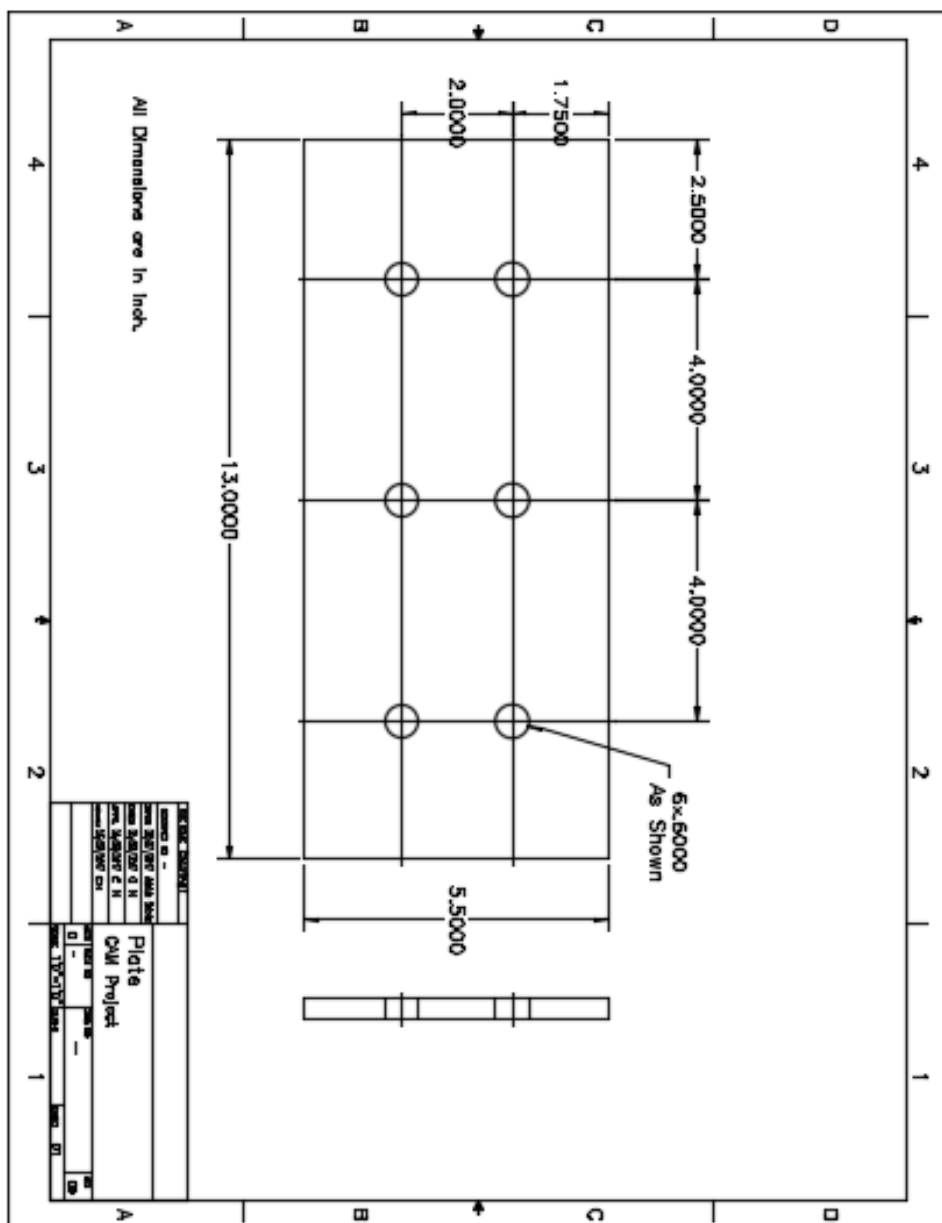†All gears have standard keyway, at 90° to setscrew.
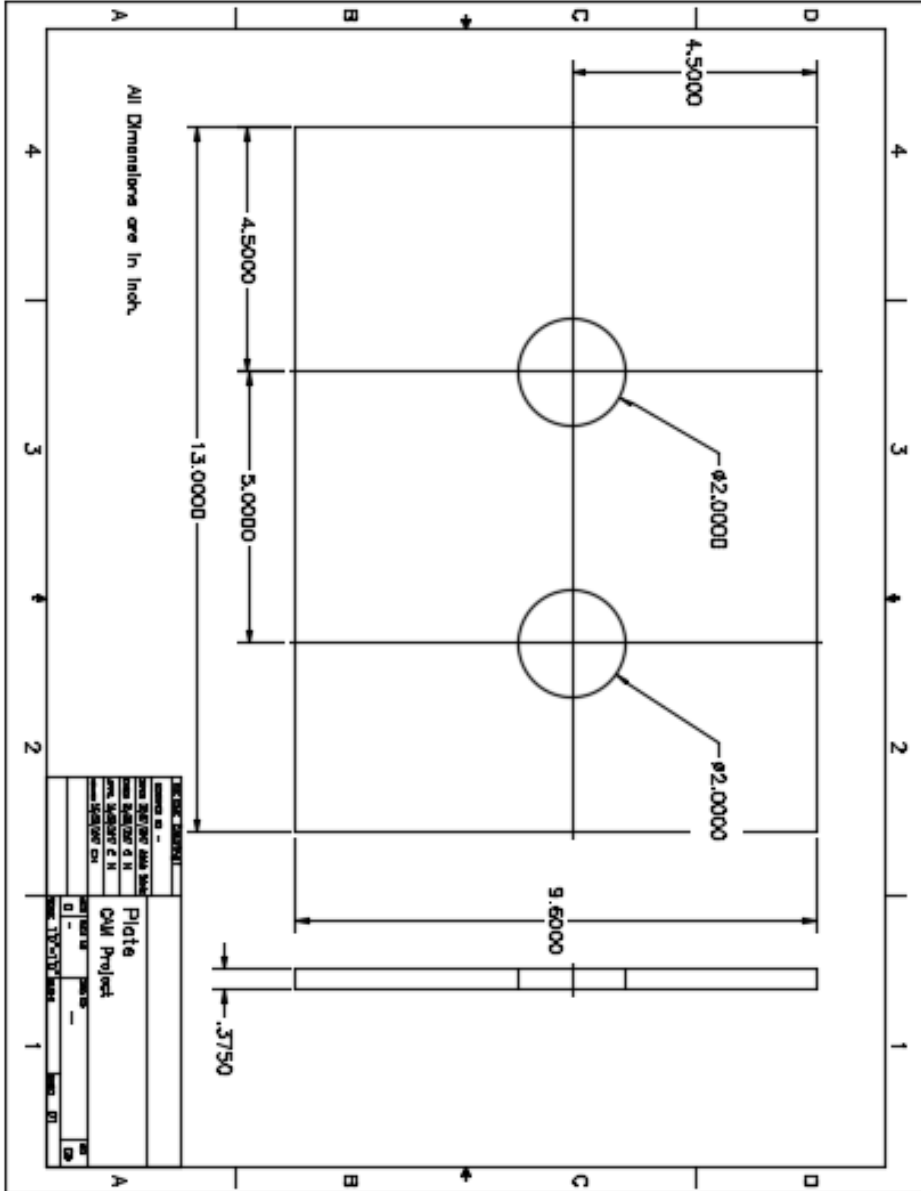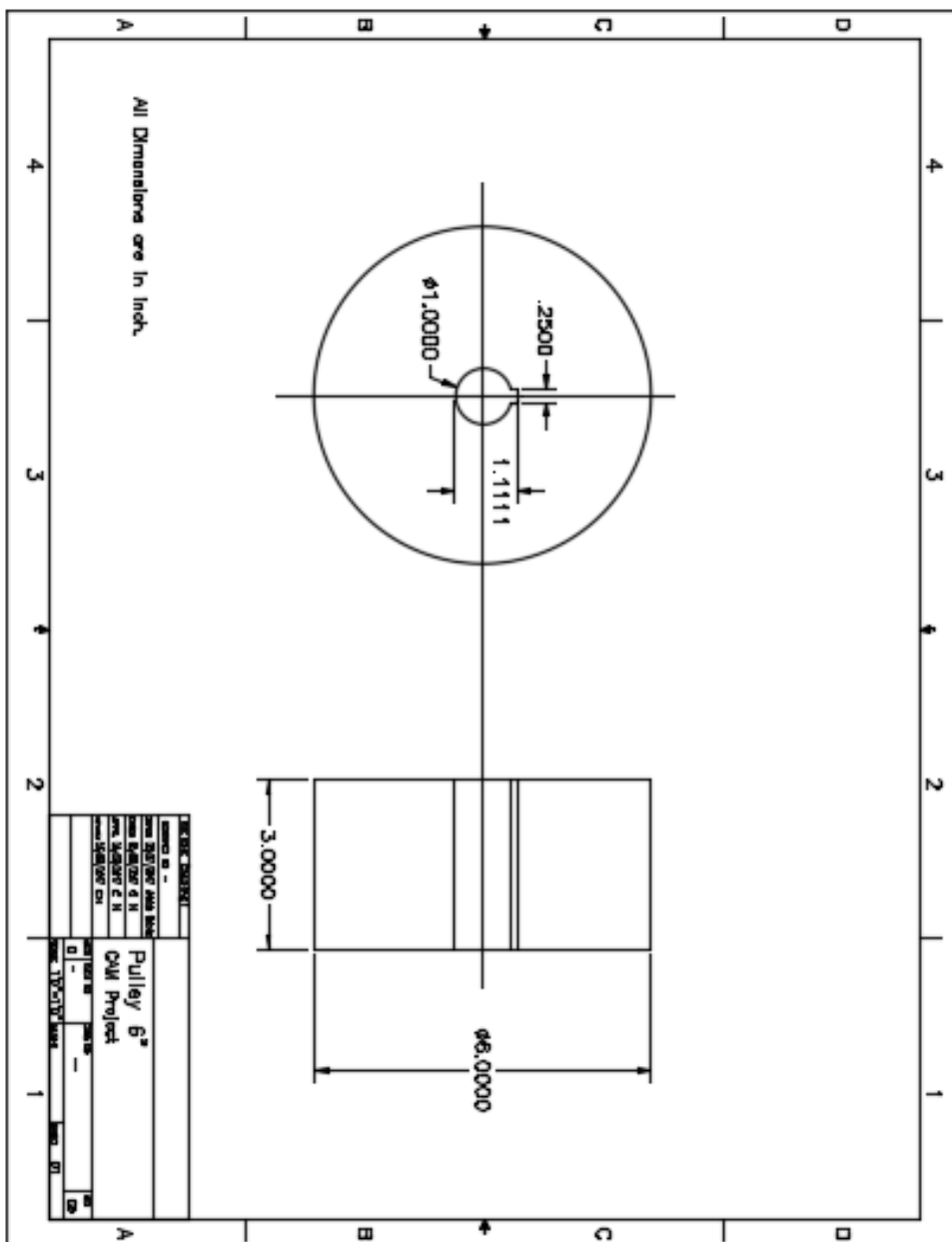
B - 2:   Gear Drawing

B - 3:   Gear Box Frame

B - 4:   Gear Box Frame (3D)

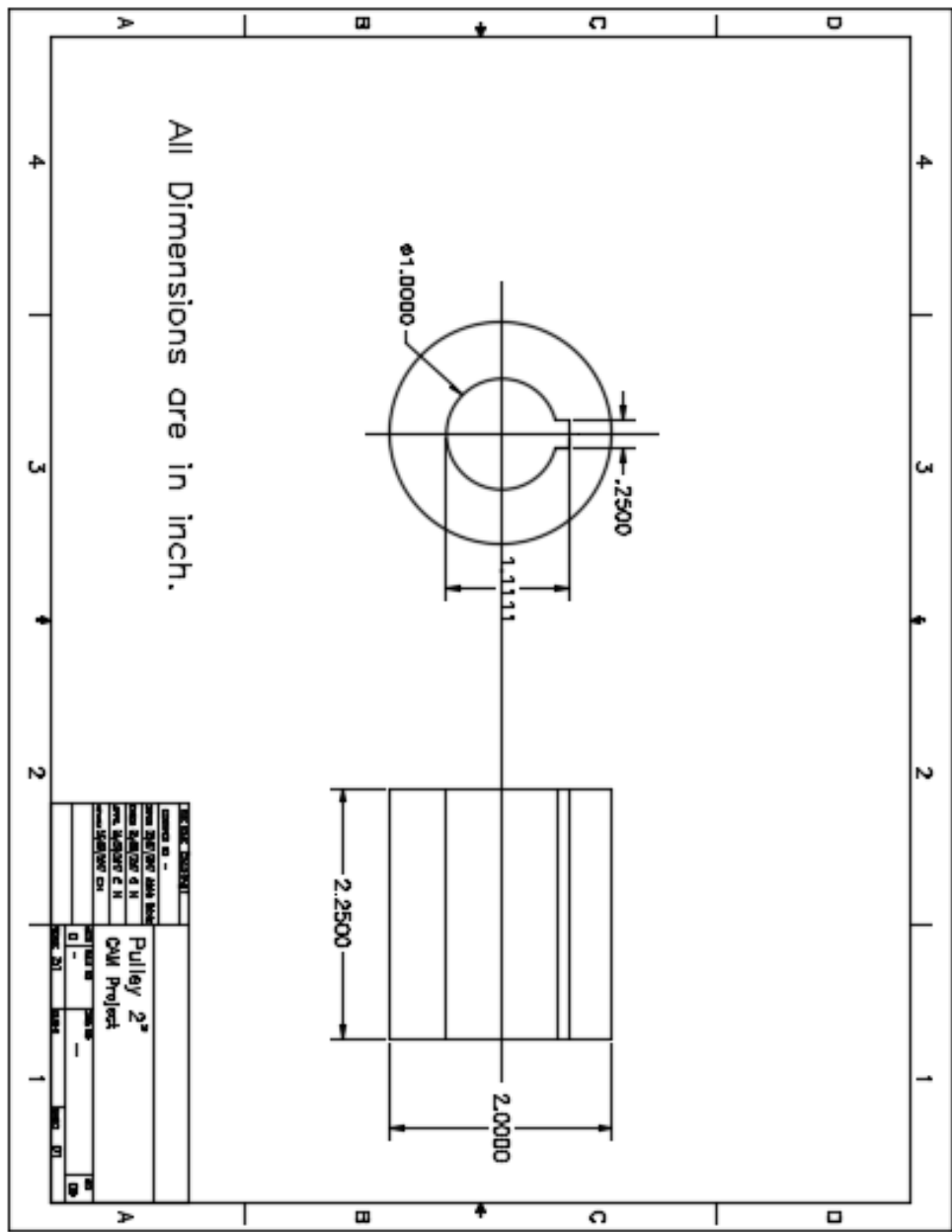**B - 5: Gear Box Plate 1 (2D drawing)**

88

B - 6:   Gear Box Plate 2 (2D drawing)

89

B - 7:   6" Spool (2D drawing)

B - 8: 2" Spool (2D Drawing)

All Dimensions are in inch.

φ1.0000

.2500

1.1111

2.2500

2.0000

Pulley 2"
CAM Project

B - 9:   Gear Box Shaft

1/8"
Key
Depth

1/4"
Key Width

12"

15/16"   -0.0010
          -0.0025

Straightness Tolerance is 0.012" per Foot

McMASTER-CARR CAD.
http://www.mcmaster.com
© 2012 McMaster-Carr Supply Company
Information in this drawing is provided for reference only.

PART
NUMBER **1497K191**

Fully Keyed
Drive Shaft
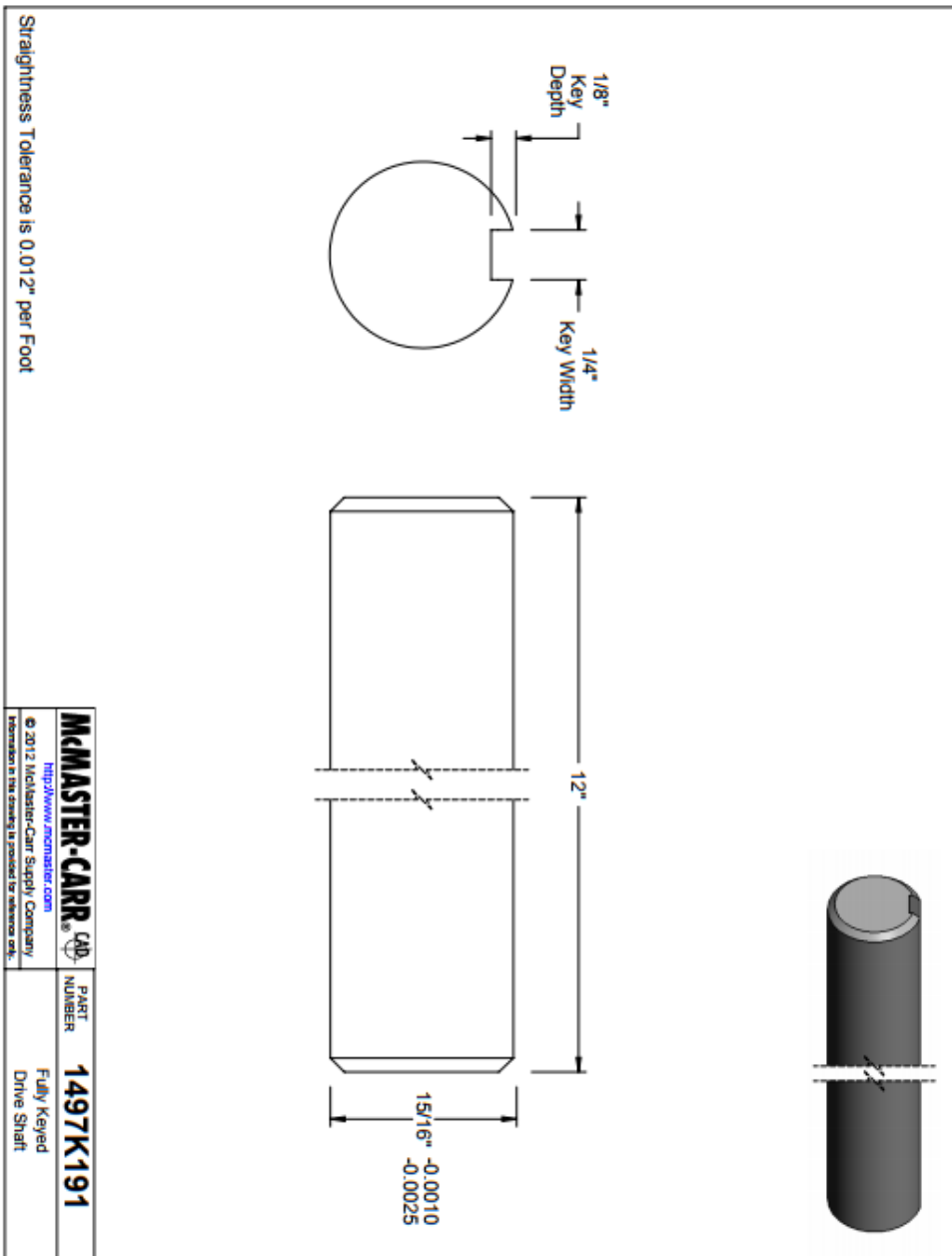
B - 10: Gear Box

B - 11: Flanged Bearing

http://www.mcmaster.com

McMASTER-CARR

PART NUMBER	6383K257
	Flanged Ball Bearing

Trade Number: 1632

2 1/8"

2" +0.002 / -0.002

1" +0.004 / -0.001

For 1" Shaft Diameter
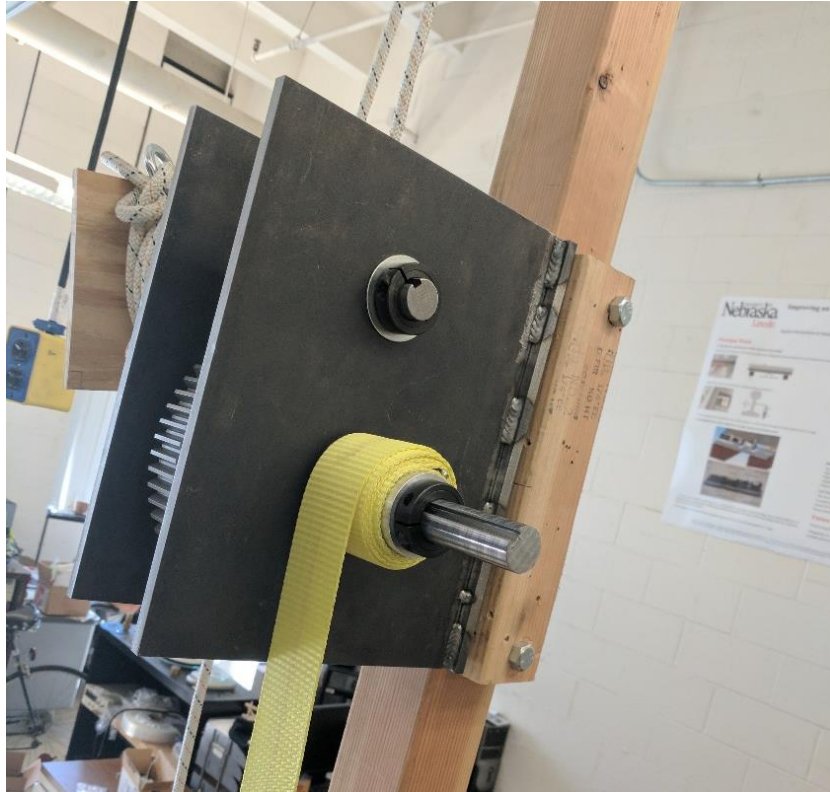
9/16"

1/16"

1/2" +0.01 / -0.01
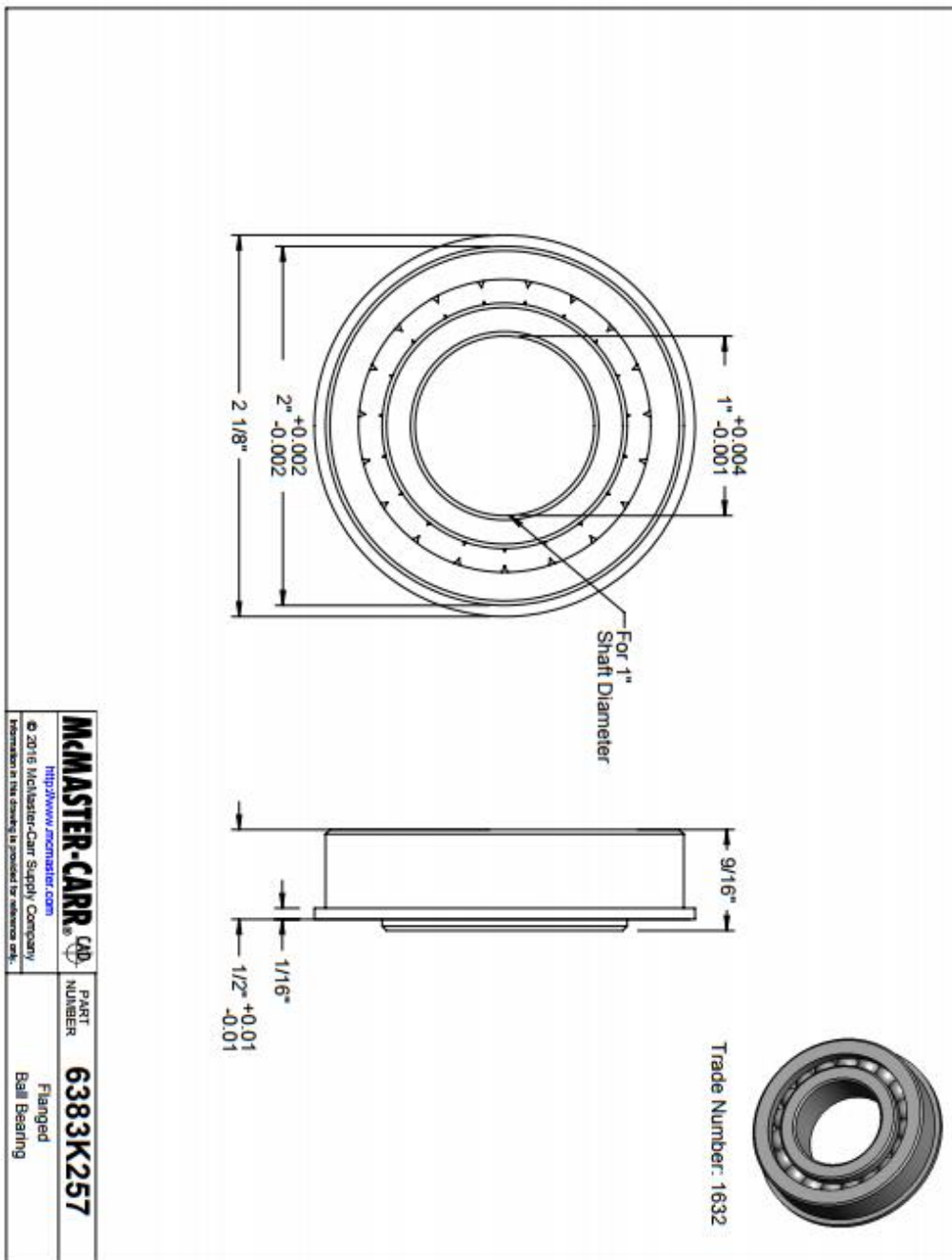
Appendix C –Counterweight Arm

C - 1: Counterweight Arm (2D Drawing)
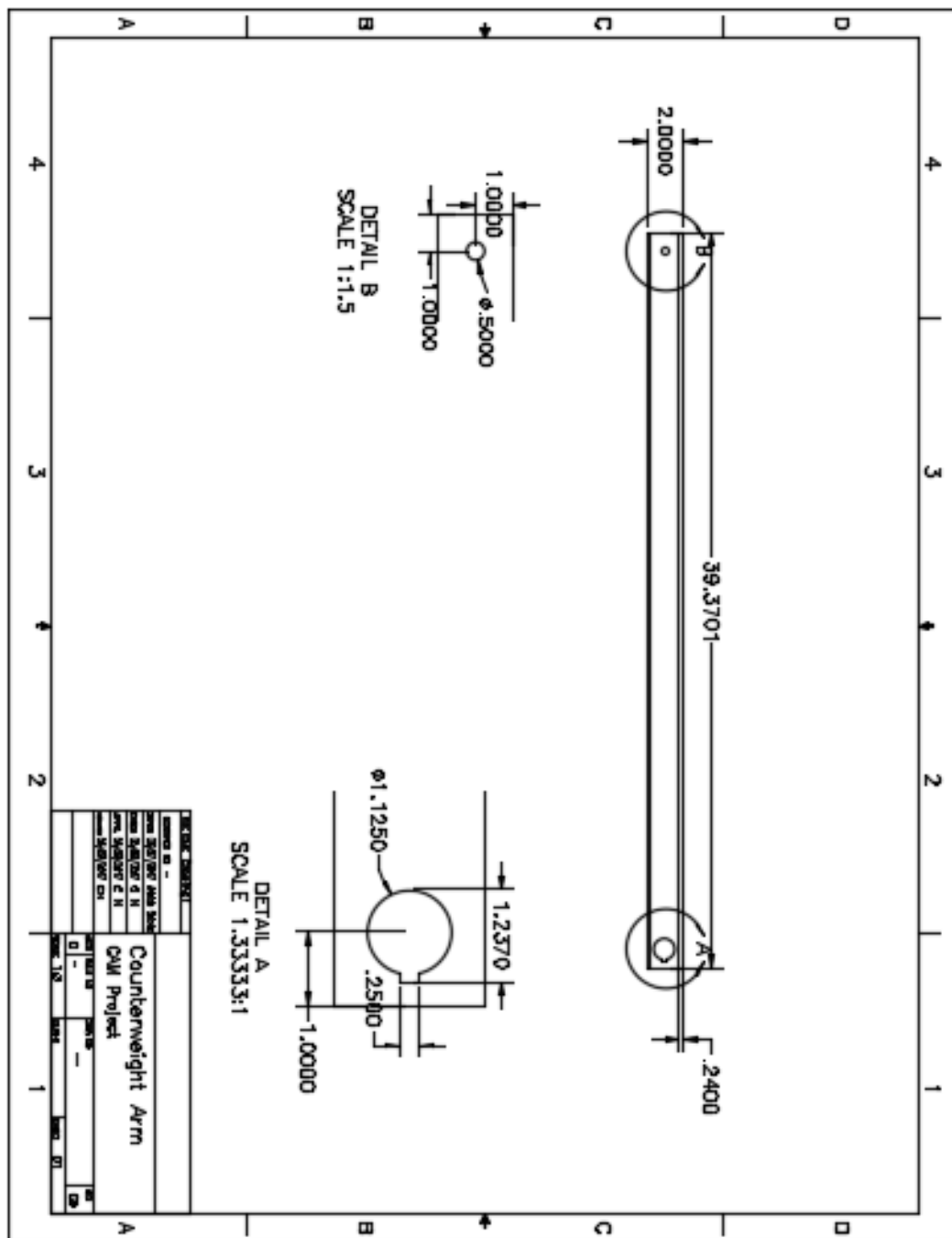
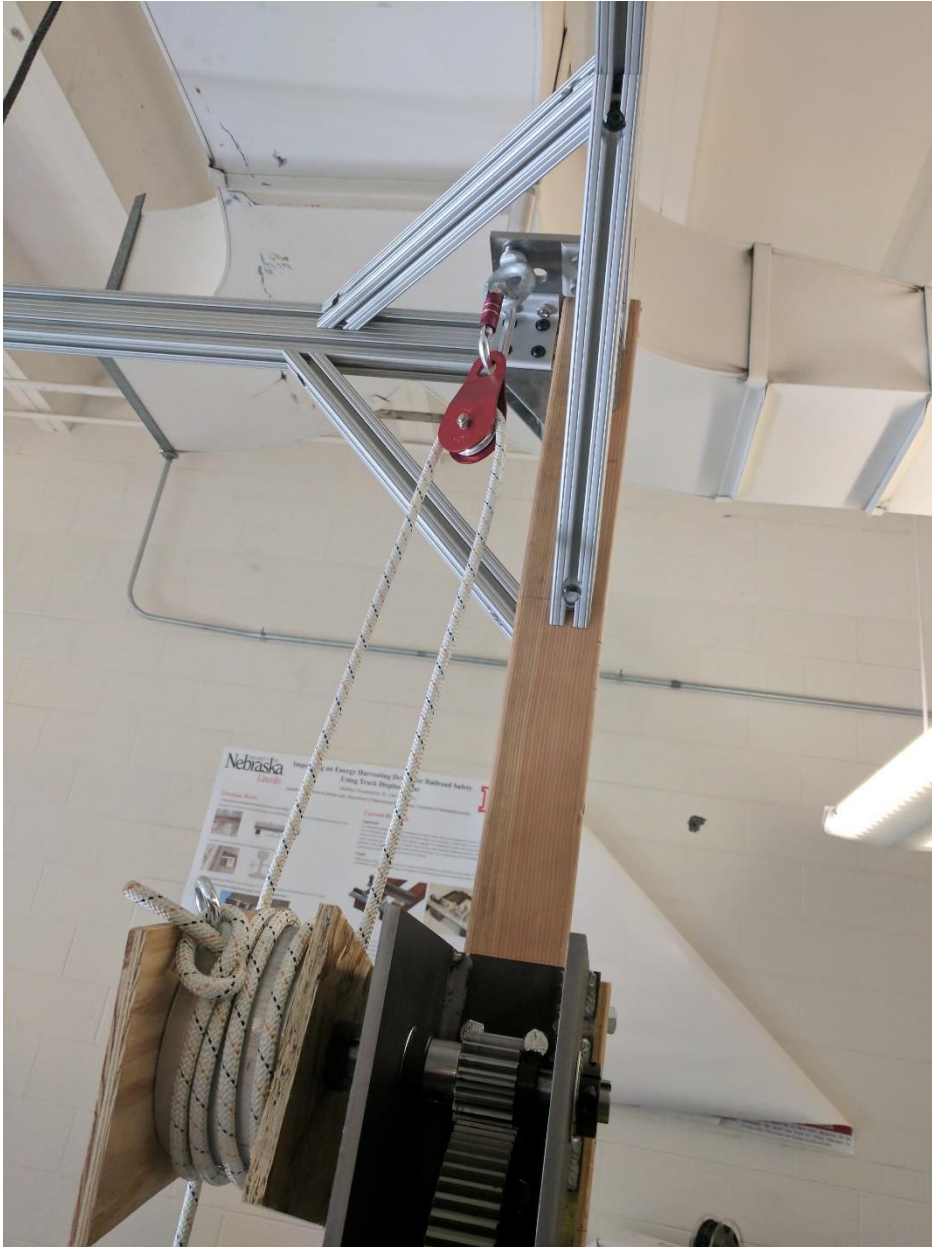# Appendix D –Test Setup (JPEG Images)

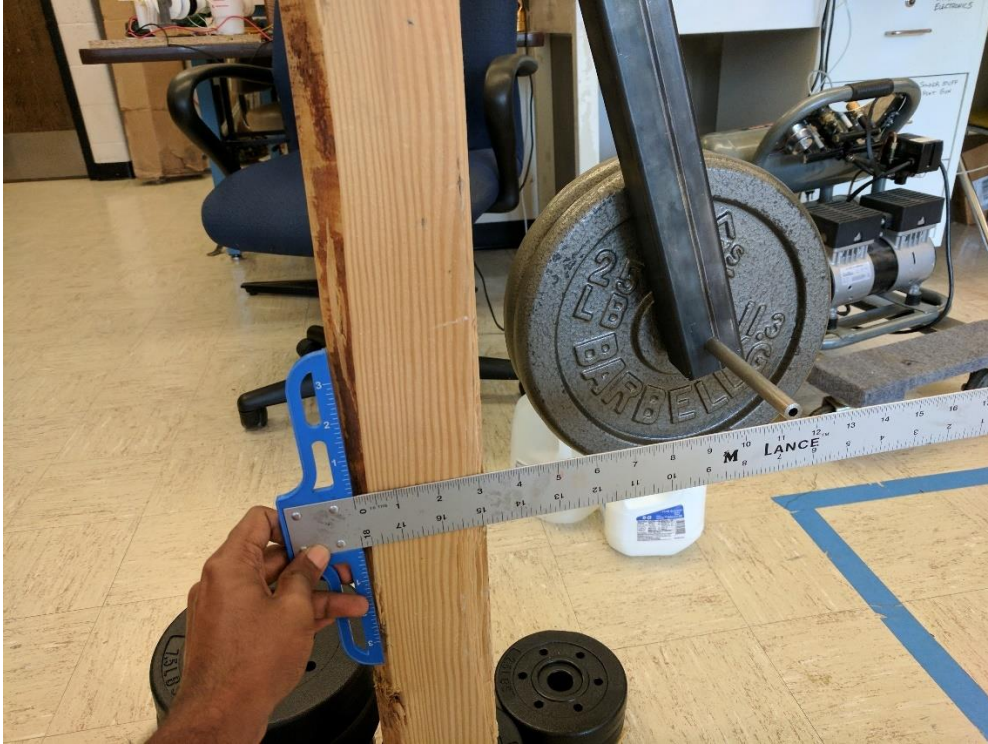**D - 1: Gear Box**

D - 2: Cam & Counterweight Arm

D - 3:   Rope connecting pulley and larger spool

D - 4:   Complete setup

D - 5: Measurement of theta (counterweight arm angle with vertical)

D - 6: Measurement of Tension in rope